

Spin-charge transport driven by magnetization dynamics on disordered surface of doped topological insulators

K. Taguchi, K. Shintani, and Y. Tanaka

*Department of Applied Physics, Nagoya University, Nagoya, 464-8603, Japan
and CREST, Japan Science and Technology Corporation (JST), Nagoya 464-8603, Japan*

(Dated: March 4, 2022)

Abstract

We theoretically study the spin and charge generation along with the electron transport on a disordered surface of a doped three-dimensional topological insulator/magnetic insulator junction by using Green's function techniques. We find that the spin and charge current are induced by not only local but also by nonlocal magnetization dynamics through nonmagnetic impurity scattering on the disordered surface of the doped topological insulator. We also clarify that the spin current as well as charge density are induced by spatially inhomogeneous magnetization dynamics, and the spin current diffusively propagates on the disordered surface. Using these results, we discuss both local and nonlocal spin torques before and after the spin and spin current generation on the surface, and provide a procedure to detect the spin current.

I. INTRODUCTION

In spintronics, the mutual control of the direction and the flow of spin is a central issue for wide applications. The flow of spin, i.e., spin current, is the difference between the currents of up and down-spin conduction electrons. It is known that the spin current is induced in the setup of the ferromagnetic metal (FM)/normal metal (NM) junction¹⁻³. Its origin is due to the magnetization dynamics in ferromagnet, which transfers the spin angular momentum of the magnetization into that of the conduction electrons. The transfer of the spin angular momentum is called spin-pumping. Here, the spin-pumping of magnetization dynamics generates the spin-current in the NM, and the spin-current can be converted into charge current through spin-orbit interactions¹⁻⁵.

Topological insulator (TI) is a new class of materials which has a gapless surface state, dubbed as the helical surface state, in which the spin and momentum are locked by the spin-orbit interactions⁶⁻⁸. On the surface of the TI, the direction of charge current and that of the spin of conduction electrons can be mutually manipulated by an applied electromagnetic field through the spin-momentum locking. There have been many theoretical works in hybrid systems including superconducting junctions on the surface of TI stimulated by the exotic surface state^{7,9-12}. In the TI/FM junctions, the anomalous charge-spin transport¹²⁻¹⁵, the anomalous tunnel conductance¹⁶⁻²⁰, the giant magneto resistance²¹⁻²³, and the current-induced spin-transfer torque^{24,25} have been studied up to now. The exotic phenomena are triggered in the presence of static magnetization and an applied electromagnetic field. The magnetization of the ferromagnet plays the role of an effective vector potential for conduction electrons, which is like a vector potential of electromagnetic fields. Owing to the effective vector potential, the time-derivative of the magnetization can be regarded as an effective electric field, and the magnetization dynamics generates charge current on the surface of the TI/FM junction even in the absence of electromagnetic fields²⁶⁻²⁹. This is called as the spin-charge conversion. The direction of the induced charge current is perfectly perpendicular to the magnetization dynamics due to the spin-momentum locking. The relation between the direction of the magnetization and the induced charge current can be a characteristic property on the surface of the TI. The property of the spin-pumping on the surface of TI can be applicable for spintronics devices.

Existing works of the spin-charge conversion have been done in the case of a clean sur-

face of the TI, namely the ballistic transport regime. However, the actual charge transport on the surface of the TI is in the diffusive regime due to the nonmagnetic impurity scattering^{21–25,30–32}. Since Burkov et al., have predicted not only the local but also the non-local current on the disordered surface of the TI in the presence of the applied electric field²¹; we can naturally expect nonlocal current is driven by the magnetization dynamics even on the disordered surface of the TI in the presence of the magnetization dynamics.

In this article, we study the charge-spin transport due to the magnetization dynamics on the disordered surface of the three-dimensional doped TI/magnetic insulator (MI) junction, as shown in Fig. 1, where we show that charge current and spin polarization on the surface of the TI are induced not only by a local, but also by a nonlocal magnetization dynamics. Besides this, we clarify that the spin current is driven by the dynamics of the spatially inhomogeneous magnetization, and the spin current diffusively propagates on the surface. The magnitude of the spin current reflects the spatially inhomogeneous spin structure of the MI. The directions of the spin flow and the spin projection of the spin current are perfectly linked by the spin-momentum locking on the surface of TIs. The present features may serve as a guide to fabricate future spintronics devices based on the surface of TIs with magnetic substance.

The merit of the choice of MI on the surface of the TI instead of metallic ferromagnet is to prevent the induced charge current going through the bulk of the MI. Then, we can focus on the charge transport on the surface of TI. Besides, the Gilbert damping constant in MIs tends to be smaller than that in ferromagnetic metals. The small value of the damping in MIs can be useful for the detection of the spin current on the disordered surface of the TI, as discussed in sec. V C

II. MODEL

We consider conduction electrons coupled to an effective localized spin on the disordered surface of the three-dimensional doped TI attached with the MI, as shown in Fig. 1. The setup in Fig. 1 is similar to a system, where conduction electrons couple with the magnetic moments of ferromagnetic metals deposited on the surface of the TI^{12,16,17}. We expect that on the surface of the TI, the effective localized spin (\mathbf{S}) can be produced from the magnetization in the MI through magnetic proximity effects. In the following, we use the

Hamiltonian, describing the surface of the TI with MI, given by

$$\mathcal{H} = \mathcal{H}_{\text{TI}} + \mathcal{H}_{sd} + V_{\text{imp}}, \quad (1)$$

where the first term in Eq. (1), \mathcal{H}_{TI} is Hamiltonian of the conduction electrons on one of the surface of the doped TI without \mathbf{S} as

$$\mathcal{H}_{\text{TI}} = \int d\mathbf{x} \psi^\dagger [-i\hbar v_F (\hat{\boldsymbol{\sigma}} \times \nabla)_z - \epsilon_F] \psi, \quad (2)$$

Here, $\psi^\dagger \equiv \psi^\dagger(\mathbf{x}, t) = (\psi_\uparrow^\dagger \ \psi_\downarrow^\dagger)$, and ψ are the creation and annihilation operators of the conduction electron, respectively (where indices \uparrow and \downarrow represent spin), ϵ_F is the Fermi energy, and v_F is the Fermi velocity of the bare electron on the surface of the doped TI. The $\hat{\boldsymbol{\sigma}}$ is the Pauli matrices in spin space. The second term of Eq. (1), \mathcal{H}_{sd} , shows the exchange interaction between the conduction electron spin $\mathbf{s} = \frac{1}{2}\psi^\dagger \boldsymbol{\sigma} \psi$ and the localized spin \mathbf{S} on the disordered surface of the doped TI, as described by

$$\mathcal{H}_{sd} = - \int d\mathbf{x} J_{sd} \psi^\dagger \mathbf{S} \cdot \hat{\boldsymbol{\sigma}} \psi, \quad (3)$$

where $J_{sd} > 0$ is the exchange coupling constant. The localized spin \mathbf{S} can be described by the magnetization of the MI as $\mathbf{S} = -(S/M)\mathbf{M}$, where S and M are the magnitude of the localized spin and of the magnetization, respectively. We consider that in general, the localized spin $\mathbf{S} \equiv \mathbf{S}(\mathbf{x}, t)$ depends on the time and position on the surface of the TI. The $\mathbf{S}(\mathbf{x}, t)$ changes slowly compared with the electron transport relaxation time (τ) and varies in space compared with the electron mean-free path (ℓ). We expect that from the Eqs. (2)-(3), the in-plane component of the localized spin, $\mathbf{S}^\parallel \equiv \mathbf{S} - S^z \mathbf{z}$, can play the role of the effective vector potential for the conduction electrons on the surface. The out-of plane component of the localized spin S^z plays a role to open the energy gap of the dispersion on the surface of the doped TI. We assume that the band gap opened by S^z is smaller than the Fermi energy on the surface of the doped TI, *i.e.*, $\epsilon_F - J_{sd} S^z > 0$. The third term of Eq. (1),

$$V_{\text{imp}} = \sum_{j=1}^{N_i} \int d\mathbf{x} U_i \psi^\dagger \psi, \quad (4)$$

represents nonmagnetic impurity scattering on the disordered surface of the doped TI. The impurity scattering causes the relaxation time τ of the transport of conduction electrons on the surface of the TI. Here $U_i = u_i \delta(\mathbf{x} - \mathbf{r}_j)$ is a delta-function type potential, u_i is a potential

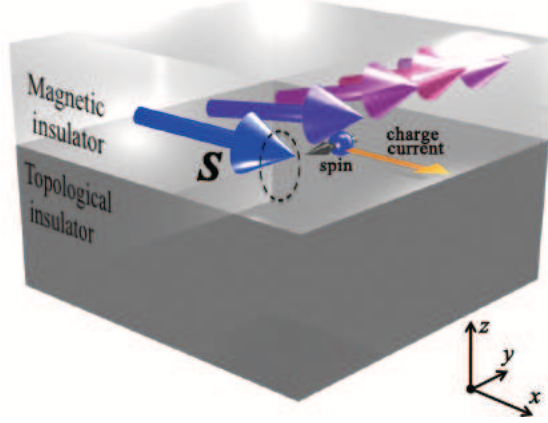


FIG. 1: (Color Online) A setup of spin-charge current generation due to magnetization dynamics in MIs deposited on disordered surface of a doped TI.

energy density, \mathbf{r}_j is the position of impurities, and N_i shows the number of impurities. The contribution of V_i can be treated by the impurity average.

We will calculate the spin current and charge current due to the spin-pumping in the linear response to \mathbf{S} under the condition $J_{sd} \ll \hbar/\tau$. We expect that the condition could be realized on a metallic disordered surface of the TI, which satisfies $\hbar/(\epsilon_F\tau) \ll 1$. For example, the exchange coupling J_{sd} can be estimated by $J_{sd} \simeq 6\text{meV}^{28}$ for $\text{Ni}_{81}\text{Fe}_{19}/\text{Bi}_2\text{Te}_3$ junction. If $\frac{\hbar}{\epsilon_F\tau} < 10^{-2}$ is satisfied, the perturbation can be accessible.

A. Renormalization of the Fermi velocity

Green's function on disordered surface of doped TI can be described by using \mathcal{H}_{TI} including V_{imp} within the self-consistent Born approximation of V_{imp} as

$$\hat{g}_{\mathbf{k},\omega} = [\hbar\omega - \{\hbar v_F(\hat{\boldsymbol{\sigma}} \times \mathbf{k})_z - \epsilon_F\} - \hat{\Sigma}_{\mathbf{k},\omega}]^{-1}, \quad (5)$$

where $\hat{\Sigma}_{\mathbf{k},\omega}$ is the self-energy within the Born approximation given by

$$\hat{\Sigma}_{\mathbf{k},\omega} = n_i \sum_{\mathbf{k}'} |u_{\mathbf{k}-\mathbf{k}'}|^2 \hat{g}_{\mathbf{k}',\omega}. \quad (6)$$

Here, $\hat{\Sigma}_{\mathbf{k},\omega}$ satisfies the Ward-Takahashi identity³³. To estimate the value of $\hat{\Sigma}_{\mathbf{k},\omega}$, we consider the \mathbf{k}' -dependence of $u_{\mathbf{k}-\mathbf{k}'}$, which plays the role to prevent the ultraviolet-divergence over a large momentum in the \mathbf{k}' -integration^{25,34}. When $\hat{\Sigma}_{\mathbf{k},\omega}$ can be described by 2×2 matrix $\hat{\Sigma}_{\mathbf{k},\omega} = \Sigma_0 + \hat{\Sigma}^{\parallel} + \Sigma^z \hat{\sigma}^z$, $\hat{\Sigma}$ is estimated, where Σ_0 and Σ^z are independent of \mathbf{k} , while

$\Sigma^{\parallel} \equiv \Sigma^x \hat{\sigma}^x + \Sigma^y \hat{\sigma}^y$ depends on \mathbf{k} . Then, the Green's function $\hat{g}_{\mathbf{k},\omega}$ is described by Σ within the Born approximation as^{25,34}

$$\hat{g}_{\mathbf{k},\omega}^r = \left[\hbar\omega - \{ \hbar\tilde{v}_F(\hat{\boldsymbol{\sigma}} \times \mathbf{k})_z - \epsilon_F \} + \frac{i\hbar}{2\tau} \right]^{-1}, \quad (7)$$

where $\hat{g}_{\mathbf{k},\omega}^r$ represents the retarded Green's function. From Eq. (7), the Fermi velocity is renormalized by Σ^{\parallel} , and the renormalized Fermi velocity is represented by $\tilde{v}_F = v_F/(1 + \xi)$, where $\xi = n_i u_0^2 / (4\pi\hbar^2 v_F^2)$ is a small value depending on the relaxation time³⁵. The last term in Eq. (7) is caused by the retarded component of $\text{Im}[\Sigma_0]$.

Equation (7) indicates the Green's function on the disordered surface of the doped TI estimated within the Born approximation of V_{imp} . Therefore, we could expect that $\hbar\tilde{v}_F(\hat{\boldsymbol{\sigma}} \times \mathbf{k})_z - \epsilon_F$ in the Eq. (7) corresponds to the dispersion on the disordered surface of the TI. The dispersion is different from that of \mathcal{H}_{TI} without V_{imp} . In the following work, we will use an effective Hamiltonian $\tilde{\mathcal{H}}_{\text{TI}}$ obtained by replacing v_F with \tilde{v}_F in Eq. (2). This replacement is needed for satisfying the charge conservation law on the disordered surface of the doped TI³⁶.

III. SPIN CURRENT DUE TO MAGNETIZATION DYNAMICS

In this section, we show spin current driven by magnetization dynamics on the disordered surface of the doped TI/MI junction. Here, the spin current and charge density are mutually related each other, because of the spin-momentum locking on the surface of the TI.

A. Definition of spin current on the surface of topological insulators

In order to derive the spin current on the disordered surface of the doped TI, we demonstrate the definition of the spin current. The spin current j_i^α is defined from

$$\partial_t s^\alpha + \nabla_i j_i^\alpha = \mathcal{T}^\alpha, \quad (8)$$

where $s^\alpha = \frac{1}{2}\langle\psi^\dagger \hat{\sigma}^\alpha \psi\rangle$ is the spin density, j_i^α shows the spin current density, and \mathcal{T}^α is the spin relaxation torque on the surface. Here the subscript and superscript of j_i^α represent the direction of flow and spin of the spin current, respectively. From Eqs. (1)-(5), j_i^α and \mathcal{T}^α are given by

$$j_i^\alpha = \frac{\tilde{v}_F}{2} \epsilon_{z\alpha i} \langle\psi^\dagger \psi\rangle = \frac{\tilde{v}_F}{2e} \epsilon_{z\alpha i} \rho_e. \quad (9)$$

with the Levi-Civita symbol $\epsilon_{z\alpha i}$. In the above equation, we used the commutation relation:

$$\begin{aligned} [\psi^\dagger, \mathcal{H}] &= -i\hbar\tilde{v}_F\epsilon_{z\alpha\ell}(\nabla_\ell\psi^\dagger)\sigma^\alpha + J_{sd}\psi^\dagger S^\alpha\sigma^\alpha, \\ [\psi, \mathcal{H}] &= -i\hbar\tilde{v}_F\epsilon_{z\alpha\ell}\sigma^\alpha(\nabla_\ell\psi) - J_{sd}S^\alpha\sigma^\alpha\psi. \end{aligned}$$

From Eq. (9), the spin current is proportional to the charge density $\rho_e = e\langle\psi^\dagger\psi\rangle$, where $e < 0$ is the charge of electrons. Moreover, the directions of the spin and flow of the spin current are perpendicular to each other because of the spin-momentum locking. The spin relaxation torque is derived from Eqs. (8)-(9). The torque can be separated as

$$\mathcal{T}^\alpha = \mathcal{T}_{\text{TI}}^\alpha + \mathcal{T}_{\text{sd}}^\alpha, \quad (10)$$

where $\mathcal{T}_{\text{TI}}^\alpha$ and $\mathcal{T}_{\text{sd}}^\alpha$ are spin relaxation torque caused by \mathcal{H}_{TI} and \mathcal{H}_{sd} , respectively. Here, $\mathcal{T}_{\text{TI}}^\alpha$ and $\mathcal{T}_{\text{sd}}^\alpha$ are given by

$$\mathcal{T}_{\text{TI}}^\alpha = \frac{i\tilde{v}_F}{2}\epsilon_{\beta z\ell}\epsilon_{\beta\alpha\nu}\langle(\nabla_\ell\psi^\dagger)\hat{\sigma}^\nu\psi - \psi^\dagger\hat{\sigma}^\nu\nabla_\ell\psi\rangle, \quad (11)$$

$$\mathcal{T}_{\text{sd}}^\alpha = \frac{2J_{sd}}{\hbar}\epsilon_{\nu\beta\alpha}s^\nu S^\beta. \quad (12)$$

We note that the definition of spin current depends on that of the spin relaxation torque³⁷⁻³⁹. For example, we consider the case when the spin relaxation torque can be described by $\tau^\alpha = \mathcal{T}^\alpha + \nabla_i\mathcal{P}_i^\alpha$, where the polarization \mathcal{P}_i^α is an arbitrary vector with $\nabla_i\mathcal{P}_i^\alpha = 0$, whose index i and α represent the direction of the polarization in the real space and that of the spin in the spin space, respectively. Then, the spin current J_i^α can be also represented by $\mathcal{J}_i^\alpha = j_i^\alpha + \mathcal{P}_i^\alpha$ and \mathcal{J}_i^α satisfies the conservation law as $\partial_t s^\alpha + \nabla_i\mathcal{J}_i^\alpha = \tau^\alpha$. We discuss the spin current defined in Eq. (9). To consider the spin current and the spin relaxation torque, we calculate the charge density and spin density in the following subsections.

B. Charge density

First, we will calculate the charge density ρ_e in the linear response to \mathbf{S} . ρ_e is described by using the lesser component of the Keldysh-Green's function, $-i\hbar G^<(\mathbf{x}, t, \mathbf{x}, t) = \langle\psi^\dagger(\mathbf{x}, t)\psi(\mathbf{x}, t)\rangle$ in the same position and time as

$$\rho_e = -i\hbar e \text{tr}[\hat{G}^<(\mathbf{x}, t, \mathbf{x}, t)]. \quad (13)$$

Hence, ρ_e is given by

$$\rho_e = \frac{i\hbar e J_{sd}}{L^2} \sum_{\mathbf{q}, \Omega} e^{i(\Omega t - \mathbf{q} \cdot \mathbf{x})} \text{tr}[\hat{\Pi}_{0\nu}(\mathbf{q}, \Omega) S_{\mathbf{q}, \Omega}^\nu], \quad (14)$$

where L^2 is the area of the disordered surface of the TI, and $\mathbf{q} = (q_x, q_y)$ and Ω indicate the momentum and frequency of the localized spin $S_{\mathbf{q}, \Omega}^\nu$ ($\nu = x, y, z$), respectively. Here, the charge-spin correlation function $\hat{\Pi}_{0\nu}$ is given by

$$\hat{\Pi}_{0\nu}(\mathbf{q}, \Omega) = \sum_{\mathbf{k}, \omega} [\hat{g}_{\mathbf{k} - \frac{\mathbf{q}}{2}, \omega - \frac{\Omega}{2}} \hat{\Lambda}_\nu(\mathbf{q}, \Omega) \hat{g}_{\mathbf{k} + \frac{\mathbf{q}}{2}, \omega + \frac{\Omega}{2}}]^\prec, \quad (15)$$

where $\hat{g}_{\mathbf{k} \pm \frac{\mathbf{q}}{2}, \omega \pm \frac{\Omega}{2}}$ is the non-perturbative Green's function of \mathcal{H}_{TI} including V_i , which is taken into account within the Born approximation. The retarded (advanced) Green's function $\hat{g}_{\mathbf{k}, \omega}^r$ ($\hat{g}_{\mathbf{k}, \omega}^a = [\hat{g}_{\mathbf{k}, \omega}^r]^\dagger$) is given by

$$\hat{g}_{\mathbf{k}, \omega}^r = [\hbar\omega + \epsilon_F - \hbar\tilde{v}_F \hat{\boldsymbol{\sigma}} \cdot (\mathbf{k} \times \mathbf{z}) + i\hbar/(2\tau)]^{-1},$$

where $\hbar/(2\tau) = \pi n_i u_i^2 \nu_e / 2$ represents the self-energy due to V_i within the Born approximation. The vector $\hat{\Lambda}_\nu$ in Eq. (15) is the vertex function, which is described by

$$\hat{\Lambda}_\gamma(\mathbf{q}, \Omega) = \hat{\sigma}_\gamma + \sum_{\zeta=0,x,y,z} [\tilde{\Gamma}(\mathbf{q}, \Omega) + [\tilde{\Gamma}(\mathbf{q}, \Omega)]^2 + \dots]_{\gamma\zeta} \hat{\sigma}_\zeta. \quad (16)$$

Here $\hat{\sigma}_0 = \hat{1}_{2 \times 2}$ is the identity matrix and $\tilde{\Gamma}_{\gamma\zeta}$ is given by $\hat{\Gamma}_\gamma$:

$$\begin{aligned} \hat{\Gamma}_\gamma(\mathbf{q}, \Omega) &\equiv n_i u_i^2 \sum_{\mathbf{k}} \hat{g}_{\mathbf{k} - \frac{\mathbf{q}}{2}, \omega - \frac{\Omega}{2}} \hat{\sigma}_\gamma \hat{g}_{\mathbf{k} + \frac{\mathbf{q}}{2}, \omega + \frac{\Omega}{2}} \\ &= \tilde{\Gamma}_{\gamma\zeta} \hat{\sigma}_\zeta. \end{aligned} \quad (17)$$

The correlation function $\hat{\Pi}_{0\nu}$ can be decomposed into the retarded and advanced Green's function by using the formula $\hat{g}_{\mathbf{k}, \omega}^\prec = f_\omega (\hat{g}_{\mathbf{k}, \omega}^a - \hat{g}_{\mathbf{k}, \omega}^r)^{40}$, where f_ω is the Fermi distribution function. Using the formula, we can estimate the correlation function $\hat{\Pi}_{0\nu}$ on the surface of the doped TI, *i.e.*, $\hbar/(\epsilon_F \tau) \ll 1$ regime as $\hat{\Pi}_{0\gamma} = \hat{\Pi}_{0\gamma}^{\text{ra}} + o(\hbar/(\epsilon_F \tau))$, where $\hat{\Pi}_{0\gamma}^{\text{ra}}$ is represented by

$$\hat{\Pi}_{0\gamma}^{\text{ra}} = \sum_{\mathbf{k}, \omega} (f_{\omega + \frac{\Omega}{2}} - f_{\omega - \frac{\Omega}{2}}) \hat{g}_{\mathbf{k} - \frac{\mathbf{q}}{2}, \omega - \frac{\Omega}{2}}^r \hat{\Lambda}_\gamma^{\text{ra}} \hat{g}_{\mathbf{k} + \frac{\mathbf{q}}{2}, \omega + \frac{\Omega}{2}}^a. \quad (18)$$

Here $\hat{\Lambda}_\gamma^{\text{ra}}$ is given by the Pauli matrix as

$$\hat{\Lambda}_\gamma^{\text{ra}} = \sum_{\zeta=0,x,y,z} [\hat{1} + \tilde{\Gamma}^{\text{ra}} + (\tilde{\Gamma}^{\text{ra}})^2 + \dots]_{\gamma\zeta} \hat{\sigma}_\zeta \equiv \sum_{\zeta} \tilde{\Lambda}_{\gamma\zeta}^{\text{ra}} \hat{\sigma}_\zeta, \quad (19)$$

$$\hat{\Gamma}_\gamma^{\text{ra}} = n_i u_i^2 \sum_{\mathbf{k}} \hat{g}_{\mathbf{k} - \frac{\mathbf{q}}{2}, \omega - \frac{\Omega}{2}}^r \hat{\sigma}_\gamma \hat{g}_{\mathbf{k} + \frac{\mathbf{q}}{2}, \omega + \frac{\Omega}{2}}^a. \quad (20)$$

Using Eqs. (19)-(20) under the condition $\Omega\tau \ll 1$, we can calculate $\hat{\Pi}_{0\gamma}^{\text{ra}}$ in the low-temperature limit. Besides this, we can calculate the response function $\hat{\Pi}_{0\gamma}^{\text{ra}}$ by postulating $\Omega\tau \ll 1$, $q\ell \ll 1$, and $q_x^2 = q_y^2 = q^2/2$. $\hat{\Pi}_{0\gamma}^{\text{ra}}$ is given by

$$\hat{\Pi}_{0\gamma}^{\text{ra}} = \frac{-\Omega}{2\pi} \sum_{\zeta=0,x,y,z} \hat{\Gamma}_{\zeta}^{\text{ra}} \tilde{\Lambda}_{\gamma\zeta}^{\text{ra}}, \quad (21)$$

where $\hat{\Gamma}_{\zeta}^{\text{ra}} \equiv \sum_{\nu=0,x,y,z} \tilde{\Gamma}_{\zeta\nu}^{\text{ra}} \sigma_{\nu}$ can be expressed by 4×4 matrix $\tilde{\Gamma}^{\text{ra}}$ as

$$\tilde{\Gamma}^{\text{ra}} = \begin{pmatrix} 1 - i\Omega\tau - \frac{1}{2}\ell^2 q^2 & \frac{i}{2}\ell q_y & -\frac{i}{2}\ell q_x & 0 \\ \frac{i}{2}\ell q_y & \frac{1}{2}(1 - i\Omega\tau - \frac{1}{2}\ell^2 q^2) & \frac{1}{4}\ell^2 q_x q_y & -\frac{i}{4}q_x \ell \frac{\hbar}{\epsilon_F \tau} \\ -\frac{i}{2}\ell q_x & \frac{1}{4}\ell^2 q_x q_y & \frac{1}{2}(1 - i\Omega\tau - \frac{1}{2}\ell^2 q^2) & -\frac{i}{4}q_y \ell \frac{\hbar}{\epsilon_F \tau} \\ 0 & \frac{i}{4}q_x \ell \frac{\hbar}{\epsilon_F \tau} & \frac{i}{4}q_y \ell \frac{\hbar}{\epsilon_F \tau} & o(\frac{\hbar}{\epsilon_F \tau})^2 \end{pmatrix}. \quad (22)$$

In the above equation, we have used $n_i u_i^2 \pi \nu_e / (\hbar/2\tau) = 1/2$. Here, $\nu_e = \epsilon_F / (2\pi \hbar^2 v_F^2)$ is the density of states at the Fermi energy on the surface of the doped TI. From the above equation, the magnitudes of $\tilde{\Gamma}_{\zeta z}$ and $\tilde{\Gamma}_{z\zeta}$ are negligibly smaller than that of $\tilde{\Gamma}_{\nu\mu}(\nu, \mu = 0, x, y)$ for $\hbar/(\epsilon_F \tau) \ll 1$. As a result, $\hat{\Gamma}_{\mu} = \sum_{\nu=0,x,y} [\tilde{\Gamma}]_{\mu\nu} \hat{\sigma}_{\nu} + o(\hbar/(\epsilon_F \tau))$ is obtained by

$$\hat{\Gamma}_0^{\text{ra}} = \left(1 - i\Omega\tau - \frac{1}{2}\ell^2 q^2\right) \hat{\sigma}_0 + \frac{i}{2} \ell \hat{\sigma}_a q_b \epsilon_{abz}, \quad (23)$$

$$\hat{\Gamma}_{\mu=x,y}^{\text{ra}} = \left[\frac{1}{2} \left(1 - i\Omega\tau - \frac{3}{4}\ell^2 q^2\right) \delta_{\mu\nu} + \frac{1}{4}\ell^2 q_{\mu} q_{\nu}\right] \hat{\sigma}_{\nu} + \frac{i}{2} \ell q_a \epsilon_{\mu az} \hat{\sigma}_0. \quad (24)$$

Then, $\tilde{\Lambda}_{\zeta\gamma}^{\text{ra}}$ can also be estimated by using $\tilde{\Gamma}^{\text{ra}}$ as⁴¹

$$\tilde{\Lambda}_{\gamma\zeta}^{\text{ra}} = [(1 - \tilde{\Gamma}^{\text{ra}})^{-1}]_{\gamma\zeta}. \quad (25)$$

Therefore, from Eqs. (13) and (21)-(24), the charge density ρ_e is obtained by

$$\begin{aligned} \rho_e &= \frac{e\nu_e J_{sd}\tau}{L^2} \sum_{\mathbf{q}, \Omega} e^{i(\Omega t - \mathbf{q} \cdot \mathbf{x})} \frac{\ell\Omega}{q^2 \ell^2 + i\Omega\tau} (q_y S_{\mathbf{q}, \Omega}^x - q_x S_{\mathbf{q}, \Omega}^y) \\ &= -e\nu_e J_{sd}\tau \ell [\nabla \times \partial_t \langle \mathbf{S}^{\parallel} \rangle_{\text{D}}]_z, \end{aligned} \quad (26)$$

From Eq. (26), we find that the charge density ρ_e is induced by $\partial_t [\nabla \times \langle \mathbf{S}^{\parallel} \rangle_{\text{D}}]_z$. Here $\langle \mathbf{S}^{\parallel} \rangle_{\text{D}}$ is defined by the convolution of the in-plane of the localized spin \mathbf{S}^{\parallel} and a diffusion propagator function \mathcal{D} on the disordered surface of the TI as

$$\langle \mathbf{S}^{\parallel} \rangle_{\text{D}}(\mathbf{x}, t) \equiv \frac{1}{\tau} \int dt' \int d\mathbf{x}' \mathcal{D}(\mathbf{x} - \mathbf{x}', t - t') \mathbf{S}^{\parallel}(\mathbf{x}', t'), \quad (27)$$

$$\mathcal{D}(\mathbf{x}, t) = \frac{1}{L^2} \sum_{\mathbf{q}, \Omega} e^{i(\Omega t - \mathbf{q} \cdot \mathbf{x})} \frac{1}{2Dq^2 + i\Omega}, \quad (28)$$

where, $D \equiv \tilde{v}_F^2 \tau / 2$ is a diffusion constant and $\langle \mathbf{S}^\parallel \rangle_D$ denotes the nonlocal spin, which diffusively propagates by the diffusion propagator \mathcal{D} . The \mathcal{D} results because of nonmagnetic impurity scattering on the disordered surface of the doped TI. We also find that the charge density due to the out-of plane of the localized spin, S^z , is negligible smaller than that due to \mathbf{S}^\parallel .

The diffusion propagator \mathcal{D} satisfies the differential equation

$$(\partial_t - 2D\nabla^2)\mathcal{D}(\mathbf{x} - \mathbf{x}', t - t') = \delta(\mathbf{x} - \mathbf{x}')\delta(t - t'). \quad (29)$$

We find that from Eqs. (26) and (27), the diffusive motion of the charge density obeys the diffusion equation:

$$(\partial_t - 2D\nabla^2)\rho_e = -e\nu_e J_{sd}\ell(\nabla \times \partial_t \mathbf{S}^\parallel)_z. \quad (30)$$

The above equation means that the diffusion propagator of the charge density is caused by the spatial and time derivative of the localized spin, $(\nabla \times \partial_t \mathbf{S}^\parallel)_z$, on the surface of the doped TI. When the localized spin is spatially uniform, ρ_e is not driven by the magnetization dynamics.

C. Spin current

We will now consider the spin current due to the magnetization dynamics on the disordered surface of the doped TI. The spin current is proportional to the charge density [see Eq. (9)]. From the result of the charge density due to magnetization dynamics [see Eq. (26)], the spin current is given by

$$j_i^\alpha = -\frac{1}{2}\epsilon_{z\alpha i}\nu_e J_{sd}\ell^2[\nabla \times \partial_t \langle \mathbf{S}^\parallel \rangle_D]_z. \quad (31)$$

This is one of the main results of this paper. From Eq. (31), the direction of spin of the spin current is perfectly locked and is perpendicular to the direction of the flow of the spin current. The origin lies on the spin-momentum locking on the surface of the TI. The spin current is proportional to the coefficients, which are the density of states at Fermi energy ν_e , the s - d exchange coupling J_{sd} , and the square of the mean-free path ℓ^2 . Here j_i^α is proportional to the spatial and time derivative of the nonlocal spin as $[\nabla \times \partial_t \langle \mathbf{S}^\parallel \rangle_D]_z$. We find that the local spin does not contribute to the spin current generation. In the case

when the spin structure of the MI is spatially uniform, the spin current vanishes. Since the spin current is proportional to the charge density, we expect that the spin current can be arising from the accumulation of the diffusive charge density, which is given by Eq. (30). Additionally, Eq. (31) indicates that the spin current is an even-function of \tilde{v}_F , the sign of which depends on the helicity of electron on the surface of the TI. Therefore, the direction of the spin and flow of the spin current on top surface ($j_{i,\text{top}}^\alpha$) and that on bottom surface of the TI ($j_{i,\text{bottom}}^\alpha$) are equal as $j_{i,\text{top}}^\alpha = j_{i,\text{bottom}}^\alpha$. We find that the in-plane component of the localized spin $\mathbf{S}^\parallel \equiv \mathbf{S} - S^z \mathbf{z}$ contributes to the spin current, but the out-of plane component of the localized spin $S^z \mathbf{z}$ does not. We expect that its origin lies on the spin-orbit coupling of \mathcal{H}_{TI} . From $(\hat{\boldsymbol{\sigma}} \times \mathbf{p})_z = \hat{\boldsymbol{\sigma}} \cdot (\mathbf{p} \times \mathbf{z})$ and $\mathbf{S}^\parallel = (\mathbf{z} \times \mathbf{S}^\parallel) \times \mathbf{z}$, the Hamiltonian $\mathcal{H}_{\text{TI}} + \mathcal{H}_{sd}$ can be described by

$$\mathcal{H}_{\text{TI}} + \mathcal{H}_{sd} = \int d\mathbf{x} \psi^\dagger \left\{ \tilde{v}_F \hat{\boldsymbol{\sigma}} \cdot \left[\left(\mathbf{p} - \frac{J_{sd}}{\tilde{v}_F} (\mathbf{z} \times \mathbf{S}^\parallel) \right) \times \mathbf{z} \right] - J_{sd} S^z \hat{\sigma}^z - \epsilon_F \right\} \psi \quad (32)$$

From the above equation, we can regard that the conduction electrons momentum \mathbf{p} is shifted by the in-plane localized spin \mathbf{S}^\parallel : $\mathbf{p} \rightarrow \mathbf{p} - \frac{J_{sd}}{\tilde{v}_F} (\mathbf{z} \times \mathbf{S}^\parallel)$. The in-plane localized spin $\mathbf{z} \times \mathbf{S}^\parallel$ plays a role like an electromagnetic vector potential $\mathcal{A} = \frac{J_{sd}}{e\tilde{v}_F} (\mathbf{z} \times \mathbf{S}^\parallel)^{13,14}$. Then, the observable quantity should be proportional to the gauge invariant form: an effective electric field $\boldsymbol{\mathcal{E}} \equiv -\partial_t \mathcal{A}$ or an effective magnetic field $\boldsymbol{\mathcal{B}} = \nabla \times \mathcal{A}$, as represented by

$$\boldsymbol{\mathcal{E}} = -\frac{J_{sd}}{e\tilde{v}_F} (\mathbf{z} \times \partial_t \mathbf{S}^\parallel), \quad (33)$$

$$\boldsymbol{\mathcal{B}} = \frac{J_{sd}}{e\tilde{v}_F} \nabla \times (\mathbf{z} \times \mathbf{S}^\parallel). \quad (34)$$

The dynamics of the in-plane component of the localized spin can be regarded as the effective electromagnetic field, which acts as a driving force to trigger the motion of conduction electrons. While, the out-of plane one $S^z \mathbf{z}$ plays a role like magnetic fields for the conduction electrons and does not directly shift \mathbf{p} in the momentum space. We expect from the difference of these properties of the localized spin, the contribution from $S^z \mathbf{z}$ could be smaller than that from \mathbf{S}^\parallel .

The spin current can be represented by using the effective electric field $\boldsymbol{\mathcal{E}}$ and $\{\nabla \times [\langle \boldsymbol{\mathcal{E}} \rangle_{\text{D}} \times \mathbf{z}]\}_z = -\nabla \cdot \langle \boldsymbol{\mathcal{E}} \rangle_{\text{D}}$ as

$$j_i^\alpha = -\frac{1}{2} \epsilon_{z\alpha i} \nu_e e \tilde{v}_F \ell^2 \nabla \cdot \langle \boldsymbol{\mathcal{E}} \rangle_{\text{D}}. \quad (35)$$

From the above equation, we find that the spin current is proportional to $\nabla \cdot \langle \mathcal{E} \rangle_D$ stemming from charge density. In fact, the charge density can be represented by $\rho_e \propto \nabla \cdot \langle \mathcal{E} \rangle_D$, as shown in Eq. (26). Here, the charge density is also proportional to $\nabla \cdot \langle \mathcal{E} \rangle_D$ and is similar to the Gauss's law in Maxwell equations as $\rho_e = \epsilon \nabla \cdot \mathbf{E}$, where ϵ is a permittivity and \mathbf{E} is an applied electric field. Thus, we can interpret that the charge density and the spin current on the surface of the TI are generated by the divergence of the effective electric field. Equations (26), (31), and (35) are the main results of this section.

IV. CHARGE CURRENT DUE TO MAGNETIZATION DYNAMICS

In this section, we show charge current due to magnetization dynamics on the disordered surface of the doped TI. Because of the spin-momentum locking, the charge current is proportional to the density of the spin polarization on the surface of the doped TI. We calculate the spin density, the charge current and the resulting spin-relaxation torque.

A. Spin density

To discuss the charge current, we calculate the spin density due to the magnetization dynamics in the linear response to the localized spin. The spin density $\mathbf{s} = \frac{1}{2} \langle \psi^\dagger \hat{\boldsymbol{\sigma}} \psi \rangle$ is given by

$$s^\mu = \frac{i\hbar J_{sd}}{2L^2} \sum_{\mathbf{q}, \Omega} e^{i(\Omega t - \mathbf{q} \cdot \mathbf{x})} \text{tr}[\hat{\Pi}_{\mu\nu}(\mathbf{q}, \Omega) S_{\mathbf{q}, \Omega}^\nu], \quad (36)$$

where, $\Pi_{\mu\nu}(\mu, \nu = x, y, z)$ is the spin-spin correlation function. $\Pi_{\mu\nu}$ can be calculated within the same formalism as in the section 3.2, and is represented by $\hat{\Pi}_{\mu\nu} = \hat{\sigma}_\mu \hat{\Pi}_{0\nu}$. From the result, we can obtain the spin density \mathbf{s} . Here, \mathbf{s} can be decomposed into two terms: $\mathbf{s} = \mathbf{s}^\parallel + s^z \mathbf{z}$, where $\mathbf{s}^\parallel = \mathbf{s} - s^z \mathbf{z}$ and $s^z \mathbf{z}$ show the in-plane and out-of plane component of the spin on the disordered surface of the doped TI, respectively. We find that $s^z \mathbf{z}$ is proportional to $\partial_t S^z$, and its magnitude is negligibly smaller than that of the magnitude of \mathbf{s}^\parallel within the approximation $|s^z|/|\mathbf{s}^\parallel| \sim o[\hbar/(\epsilon_F \tau) \ll 1]$. Thus, the spin density can be estimated by $\mathbf{s} = \mathbf{s}^\parallel + o[\hbar/(\epsilon_F \tau)]$ and S^z does not contribute to the generation of \mathbf{s} . The dominant contribution of \mathbf{s} can also be decomposed into two terms:

$$\mathbf{s} = \mathbf{s}^L + \mathbf{s}^D, \quad (37)$$

where \mathbf{s}^L is the local spin density due to \mathbf{S}^\parallel , and is given by

$$\mathbf{s}^L = -\frac{1}{2}\nu_e J_{sd}\tau \partial_t \mathbf{S}^\parallel. \quad (38)$$

The local spin density \mathbf{s}^L is induced by the time-derivative of the in-plane component of the localized spin $\partial_t \mathbf{S}^\parallel$. On the other hand, the second term of Eq. (37), \mathbf{s}^D , is the diffusive spin density and is given by

$$\mathbf{s}^D = -\frac{1}{2}\nu_e J_{sd}\tau \ell^2 (\mathbf{z} \times \nabla) [\nabla \times \partial_t \langle \mathbf{S}^\parallel \rangle_D]_z \quad (39)$$

$$= \frac{\ell}{2e} (\mathbf{z} \times \nabla) \rho_e. \quad (40)$$

From Eq. (40), \mathbf{s}^D is generated by the driving field $(\mathbf{z} \times \nabla)(\nabla \times \partial_t \langle \mathbf{S} \rangle_D)_z$, which is the spatial gradient and the time-derivative of the nonlocal localized spin $\langle \mathbf{S}^\parallel \rangle_D$. The driving field is also described by $(\mathbf{z} \times \nabla)(\nabla \times \partial_t \langle \mathbf{S} \rangle_D)_z = \partial_t [\nabla^2 \langle \mathbf{S} \rangle_D - \nabla(\nabla \cdot \langle \mathbf{S} \rangle_D)]$. Here, \mathbf{s}^D is described by the spatial gradient of the charge density, which is caused by the electron diffusion on the surface of the TI, as shown in Eq. (26). In addition, \mathbf{s}^D is also represented by the spin current: The charge density is proportional to the spin current, $\rho_e = \frac{e}{v_F}(j_y^x - j_x^y)$, and \mathbf{s}^D becomes

$$\mathbf{s}^D = \frac{1}{2}\tau \epsilon_{z\alpha i} (\mathbf{z} \times \nabla) j_i^\alpha. \quad (41)$$

From Eqs. (38)-(39), we find that \mathbf{s} is an even-function of \tilde{v}_F and is independent of the helicity on the surface of the TI. Therefore, the direction of \mathbf{s} does not depend on whether we are focusing on the top or bottom surface of the TI.

We find that from Eqs. (38)-(39), the spin is polarized not by a static magnetization but by magnetization dynamics. Therefore, we expect that static magnetization does not induce spin polarization on the surface of the TI. This seems to be anomalous property on the surface. The response between the spin polarization and the static magnetization on the surface of the TI is different from that in conventional metals: In the metals, a spin is polarized even by static magnetization. We will consider shortly why static magnetization does not generate spin polarization on the surface of the TI. The magnetization on the surface of the TI plays the role to shift the momentum of conduction electrons from \mathbf{p} into $\mathbf{p} - \frac{J_{sd}}{v_F}(\mathbf{z} \times \mathbf{S}^\parallel)$ in momentum space. As a result, the center of Fermi sphere is also shifted from $\mathbf{p} = 0$ into $\mathbf{p} = \frac{J_{sd}}{v_F}(\mathbf{z} \times \mathbf{S}^\parallel)$. Then, the direction of the spin at each momentum are perfectly perpendicular to that of the momentum. Besides, the spin configuration in

momentum space does not change before and after the shift, because the direction of the spin at each momentum are independent of the shift. Therefore, no spin polarization is driven by momentum shift due to a static magnetization.

B. Charge current

We note that on the surface of the TI, the charge current \mathbf{j} is proportional to the spin density on the surface of the TI. The charge current is represented by using the renormalized velocity operator as $\mathbf{j} = 2e\tilde{v}_F(\mathbf{z} \times \mathbf{s})^{36}$. From Eqs. (38)-(40), the charge current is also decomposed into two terms: $\mathbf{j} = \mathbf{j}^L + \mathbf{j}^D$ as

$$\mathbf{j}^L = -e\nu_e J_{sd}\ell(\mathbf{z} \times \partial_t \mathbf{S}^\parallel), \quad (42)$$

$$\mathbf{j}^D = e\nu_e J_{sd}\ell^3 \nabla[\nabla \times \partial_t \langle \mathbf{S}^\parallel \rangle_D]_z. \quad (43)$$

The \mathbf{j}^L is the local charge current and is induced by the time-derivative of the localized spin \mathbf{S}^\parallel . The direction of \mathbf{j}^L is parallel to $\mathbf{z} \times \mathbf{S}^\parallel$. On the other hand, \mathbf{j}^D is the diffusive charge current caused by impurity scattering on the disordered surface of the TI. In fact, \mathbf{j}^D can be represented by the spatial gradient of the charge density as $\mathbf{j}^D = -2D\nabla\rho_e$. This means that diffusive current is generated by the spatial gradient of the charge density on the surface of the TI. We note that the charge current is an odd-function of \tilde{v}_F , so that the direction of the charge current on the top surface \mathbf{j}_{top} is opposite to that on the bottom surface $\mathbf{j}_{\text{bottom}}$, if \mathbf{S} is same on the top and bottom surface. It is noted that, from Eqs. (26) and (42)-(43), the charge density ρ_e and charge current \mathbf{j} satisfy the conservation law $\dot{\rho}_e + \nabla \cdot \mathbf{j}_\gamma = 0$. The detail is shown in Appendix B.

Next, we comment on the relationship between the spin current and the charge current on the disordered surface of the doped TI. Substituting $\epsilon_{z\alpha i} j_i^\alpha = \tilde{v}_F \rho_e / e$ into Eq. (43), we find that the diffusive charge current can be described by the spin current as

$$\mathbf{j}^D = -e\ell\epsilon_{z\alpha i} \nabla j_i^\alpha. \quad (44)$$

This is also the main result of this paper. We expect that the above equation displays the conversion between the spin current into the diffusive charge current on the disordered surface of the doped TI by using the spatial gradient of the spin current. The spin current can be converted into the diffusive charge current when the spin current depends on the

space on the disordered surface. The relation in Eq. (44) is plausible on the disordered surface of the doped TI, because the charge density ρ_e is proportional to the spin current, and a diffusive particle current generally proportional to a spatial gradient of particles. We note that there is no relation between the spin current and the local charge current \mathbf{j}^L .

C. Effective conductivity

The charge current due to magnetization dynamics \mathbf{j} can be also described by the effective electric field \mathcal{E} :

$$\mathbf{j} = e^2 \tilde{v}_F^2 \nu_e \tau \mathcal{E} + e^2 \tilde{v}_F \nu_e \ell^3 \nabla [\nabla \cdot \langle \mathcal{E} \rangle_D]. \quad (45)$$

The first term and the second term are corresponding to the local and diffusive charge current, respectively. From the above results, we will consider an effective conductivity: an efficiency of the charge flow due to the applied effective electric field \mathcal{E} . This is similar to the conventional electric conductivity: In general, the longitudinal electrical conductivity is defined from dividing the charge current by an applied electric field⁴². We expect that the current corresponds to the local current. Then, an effective longitudinal electrical conductivity can be defined by $\mathbf{j}^L = \sigma \mathcal{E}$, and is given by the first term in Eq. (45) as

$$\sigma = e^2 \tilde{v}_F^2 \nu_e \tau. \quad (46)$$

The conductivity only depends on the parameters on the surface of the TI, and is independent of parameters attached to the MI.

D. Spin relaxation torque

We will consider the spin relaxation due to the magnetization dynamics on the surface of the TI. Using Eqs. (31) and (37)-(39), we can describe $\partial_t s^\alpha$ and $\nabla_i j_i^\alpha$ as

$$\partial_t s^\alpha = -\frac{1}{2} \nu_e J_{sd} \tau \partial_t^2 S^{\parallel, \alpha} + \frac{1}{2} \nu_e J_{sd} \ell^2 \tau \epsilon_{\alpha iz} \nabla_i [\nabla \times \partial_t^2 \langle \mathbf{S}^{\parallel} \rangle_D]_z, \quad (47)$$

$$\nabla_i j_i^\alpha = -\frac{1}{2} \nu_e J_{sd} \ell^2 \epsilon_{\alpha iz} \nabla_i [\nabla \times \partial_t \langle \mathbf{S}^{\parallel} \rangle_D]_z. \quad (48)$$

Therefore, the spin relaxation torque $\mathcal{T}^\alpha = \partial_t s^\alpha + \nabla_i j_i^\alpha$ in the linear response to \mathbf{S}^{\parallel} is obtained by

$$\mathcal{T} = -\frac{1}{2} \nu_e J_{sd} \tau \partial_t^2 \mathbf{S}^{\parallel} + \frac{1}{2} \nu_e J_{sd} \ell^2 (1 - \tau \partial_t) (\mathbf{z} \times \nabla) [\nabla \times \partial_t \langle \mathbf{S}^{\parallel} \rangle_D]_z + \mathcal{O}(J_{sd}^2). \quad (49)$$

The first term in Eq. (47) shows a local spin relaxation torque and is induced by $\partial_t^2 \mathbf{S}^\parallel$. The second term is a nonlocal spin relaxation torque and is driven by $(\mathbf{z} \times \nabla)(\nabla \times \partial_t \langle \mathbf{S}^\parallel \rangle_D)_z$. The nonlocal torque vanishes when the magnetization is spatially uniform. The third term in Eq. (47) represents the higher order of J_{sd} and \mathbf{S} . From Eq. (12), the spin relaxation torque \mathcal{T}_{sd} is proportional to \mathbf{S} and \mathbf{s} , which is proportional to \mathbf{S}^\parallel . Therefore, the third term in Eq. (47) corresponds to \mathcal{T}_{sd} within the linear response to \mathbf{S} . We expect that the third term $\mathcal{T}_{sd} \simeq o(\frac{J_{sd}\tau}{\hbar})^2$ can be negligibly small and be ignored in comparison with the first and the second terms of \mathcal{T} in the regime $\frac{J_{sd}\tau}{\hbar} \ll 1$.

The spin relaxation torque \mathcal{T} is also represented by the effective electric field as

$$\mathcal{T} = \frac{1}{2} e \nu_e \tilde{v}_F \tau (\partial_t \mathcal{E} \times \mathbf{z}) + \frac{1}{2} e \nu_e \tilde{v}_F \ell^2 (1 - \tau \partial_t) (\mathbf{z} \times \nabla) [\nabla \cdot \langle \mathcal{E} \rangle_D]. \quad (50)$$

The local spin relaxation is written as the time-derivative of the effective electric field and the diffusive one is induced by the spatial gradient of the nonlocal effective electric field. The electric field dependence of the spin relaxation torque on the surface of the TI is different from that in NM with spin-orbit interactions: The spin relaxation torque in the NM, \mathcal{T}_{NM} , is proportional to the spatial gradient of the applied electric field³⁹. We expect that the difference can be caused by the \mathbf{k} -dependence of the energy dispersion: The energy dispersion on the surface of the TI is a linear function of \mathbf{k} , while that in the NM proportional to the square of \mathbf{k} . Equations (39), (44), and (46) are the main results of this section.

V. DISCUSSION

A. Spin torque

We will phenomenologically study the change of the magnetization dynamics in before and after the spin-charge generation due to the ferromagnetic resonance (FMR). Now, we consider a disordered surface of the MI/TI junction, as shown in Fig.1. Further, in the junction, a static magnetic field and ac magnetic field are additionally applied. Here ac magnetic field is given by a microwave irradiation, and is needed for FMR in the MI. When we apply this magnetic field, the magnetization dynamics is triggered in the MI, and the magnetization dynamics induces the spin polarization on the surface of the TI [see Eqs. (37)-(39)]. Then, the induced spin polarization \mathbf{s} plays the role of an exchange field acting on the magnetization in the MI. As a result, the magnetization dynamics is affected from

the generated spin \mathbf{s} . Here, the mutual interaction between the magnetization dynamics and the induced spin are called as the feedback effect²⁵.

The magnetization dynamics on the disordered surface of the doped TI is described from the Landau–Lifshitz–Gilbert (LLG) equation as⁴³

$$\partial_t \mathbf{M} = -\gamma\mu(\mathbf{M} \times \mathbf{H}) + \frac{\alpha}{M} \mathbf{M} \times \partial_t \mathbf{M} + \mathcal{T}_e, \quad (51)$$

where, $\mathbf{M} = -\frac{M}{S}\mathbf{S}$ is the magnetization of the MI, γ is the gyromagnetic ratio, μ is a permeability, α is a Gilbert damping constant, $\mathbf{H} = \mathbf{H}_0 + \mathbf{H}_{ac}$ is an applied magnetic field on the disordered surface of the doped TI. \mathbf{H}_0 and \mathbf{H}_{ac} denote a static and ac magnetic field, respectively. The spin torque on the disordered surface of the doped TI is given by $\mathcal{T}_e = \frac{2J_{sd}a^2}{\hbar}\mathbf{M} \times \mathbf{s}$. The torque can be decomposed into two terms: $\mathcal{T}_e = \mathcal{T}_e^L + \mathcal{T}_e^D$, where $\mathcal{T}_e^L = \frac{2J_{sd}a^2}{\hbar}\mathbf{M} \times \mathbf{s}^L$ and $\mathcal{T}_e^D = \frac{2J_{sd}a^2}{\hbar}\mathbf{M} \times \mathbf{s}^D$ are the local and diffusive spin torque, respectively. Here, a is a lattice constant on the surface of the TI. These spin torques are obtained from Eqs. (37)-(39) and $\mathbf{S}^{\parallel} = -\frac{S^{\parallel}}{M^{\parallel}}\mathbf{M}^{\parallel}$ as

$$\mathcal{T}_e^L = \frac{\kappa}{M^{\parallel}} \mathbf{M} \times \partial_t \mathbf{M}^{\parallel}, \quad (52)$$

$$\mathcal{T}_e^D = \frac{\kappa}{M^{\parallel}} \ell^2 \mathbf{M} \times (\mathbf{z} \times \nabla) (\nabla \times \partial_t \langle \mathbf{M}^{\parallel} \rangle_D)_z, \quad (53)$$

where, M^{\parallel} is the magnitude of the in-plane magnetization $\mathbf{M}^{\parallel} \equiv \mathbf{M} - M_z \mathbf{z}$, and $\kappa = \nu_e a^2 J_{sd}^2 \tau S^{\parallel} / \hbar$ is dimensionless coefficient proportional to J_{sd}^2 and τ . We find that $\mathcal{T}_e^L \propto \mathbf{M} \times \partial_t \mathbf{M}^{\parallel}$ is slightly different from the damping torque $\frac{\alpha}{M} \mathbf{M} \times \partial_t \mathbf{M}$; which is a damping of the magnetization. We could expect that the contribution from the local spin torque \mathcal{T}_e^L can be observed in the experiments on the surface of FM/TI junction^{27,28}. Here, \mathcal{T}_e^L plays the role of an anisotropic damping torque unless the static magnetic field and microwave are parallel to the z direction. The anisotropic damping affects the magnetic permeability: For example, when the static magnetic field and microwave are parallel to the y -direction, then, the longitudinal magnetic permeability χ_{xx} and χ_{zz} are not equal each other. Here, \mathcal{T}_e^D seems to be a new type of spin torque \mathcal{T}_e^D on the surface of the TI. \mathcal{T}_e^D in Eq. (53) is induced by the spatial gradient of the magnetization, $\mathbf{M} \times (\mathbf{z} \times \nabla) (\nabla \times \partial_t \langle \mathbf{M}^{\parallel} \rangle_D)_z$. When the magnetization is spatially uniform, \mathcal{T}_e^D is zero and \mathcal{T}_e^L is nonzero.

Since, j_i^{α} and \mathcal{T}_e^D are proportional to the charge density on the disordered surface of the doped TI, \mathcal{T}_e^D can be described by the spin current j_i^{α} :

$$\mathcal{T}_e^D = \frac{J_{sd} \tau a^2}{\hbar} \mathbf{M} \times [(\mathbf{z} \times \nabla) \epsilon_{z\alpha i} j_i^{\alpha}]. \quad (54)$$

The spatial gradient of the spin current induces the diffusive spin torque on the disordered surface of the doped TI. We expect that the contribution of j_i^α is detected from the change of the half-width value, as well as the change of a shift of the magnetic resonance frequency through \mathcal{T}_e^D [discussed in Sec.V C]. Equations (52)-(54) are the main results of this section.

B. Magnetic permeability without diffusion

Using Eqs. (51)-(53), we discuss the magnetic permeability in FMR when the magnetization is spatially uniform on the surface of the MI/TI junction. We consider that in the junction, the applied static magnetic field \mathbf{H}_0 and the microwave of the ac magnetic field \mathbf{H}_{ac} are applied along the y direction: $\mathbf{H}_0 = (0, H, 0)$ and $\mathbf{H}_{ac} = (h_x, 0, h_z)$. For an uniform magnetization case, the spin becomes $\mathbf{s}^L \neq 0$ and $\mathbf{s}^D = 0$, and the spin torque are $\mathcal{T}_e^L \neq 0$, but $\mathcal{T}_e^D = 0$.

Then, the LLG equation on the surface of the MI/TI junction can be described by

$$\partial_t \mathbf{M} = \gamma \mu (\mathbf{H} \times \mathbf{M}) + \frac{\alpha}{M} (\mathbf{M} \times \partial_t \mathbf{M}) + \frac{\kappa}{M^\parallel} (\mathbf{M} \times \partial_t \mathbf{M}^\parallel). \quad (55)$$

To estimate the magnetic permeability on the surface of the TI, we assume that the $|\mathbf{H}_0|$ is larger than the $|\mathbf{H}_{ac}|$, *i.e.*, $|h_x| \ll H$ and $|h_z| \ll H$. Then, from the applied magnetic field, we expect that the local magnetization on the surface $\mathbf{M} = (m_x, M_y, m_z)$ can be satisfied $m_x \ll M_y$ and $m_z \ll M_y$. Moreover we assume that the time-dependence of the precession of \mathbf{M} is given by $m_x \propto m_z \propto e^{i\Omega t}$ and $\partial_t M_y \sim 0$. In order to solve the LLG equation, we take a linear approximation of m_i : $m_i m_j \sim 0$, $M_y \sim M (= |\mathbf{M}|)$, and $M^\parallel \sim M$. Then, the LLG equation becomes

$$\begin{aligned} \partial_t m_x &= \gamma \mu (H m_z - h_z M) + \alpha \partial_t m_z, \\ \partial_t m_z &= \gamma \mu (h_x M - H m_x) - (\alpha + \kappa) \partial_t m_x, \end{aligned} \quad (56)$$

and the magnetic permeability is given by

$$\begin{pmatrix} m_x \\ m_z \end{pmatrix} = \begin{pmatrix} \chi_{xx} & \chi_{xz} \\ \chi_{zx} & \chi_{zz} \end{pmatrix} \begin{pmatrix} h_x \\ h_z \end{pmatrix}. \quad (57)$$

The frequency dependence of the longitudinal magnetic permeability χ_{xx} and χ_{zz} are de-

scribed by

$$\chi_{xx} = \frac{\omega_M(\omega_H + i\alpha\Omega)}{(\omega_H + i\alpha\Omega)[\omega_H + i(\alpha + \kappa)\Omega] - \Omega^2}, \quad (58)$$

$$\chi_{zz} = \frac{\omega_H + i(\alpha + \kappa)\Omega}{\omega_H + i\alpha\Omega} \chi_{xx}, \quad (59)$$

where. $\omega_H = \gamma\mu H$ and $\omega_M = \gamma\mu M$ are the angular frequency of the applied static magnetic field and that of the magnetization, respectively. The permeability χ_{xx} and χ_{zz} are different each other originating from the anisotropic spin-transfer torque \mathcal{T}_e^L . Transverse magnetic permeability has the relation $\chi_{xz} = -\chi_{zx}$ and is given by

$$\chi_{xz} = \frac{-i\Omega}{\omega_H + i\alpha\Omega} \chi_{xx}. \quad (60)$$

The real part of the permeability $\text{Re}[\chi_{xx}]$ shows a Lorentzian profile due to the magnetic resonance around the resonant frequency Ω_r , which is proportional to H . The $\text{Im}[\chi_{xx}]$ indicates the energy absorption of the applied microwave around Ω_r . Half-width value of $\text{Im}[\chi_{xx}]$ expresses the damping of the precessional motion of the magnetization. From Eq. (58), the half-width value $\Delta\Omega$ is caused by the Gilbert damping ($\alpha\mathbf{M} \times \partial_t\mathbf{M}$) and the local spin torque \mathcal{T}_e^L given by

$$\Delta\Omega \simeq (2\alpha + \kappa)\Omega_r. \quad (61)$$

We expect that in the MI without TI, the half-width value of the magnetic permeability estimates $\Delta\Omega = 2\alpha\Omega_r$. Eq. (61) indicates that on the surface of the doped TI, $\Delta\Omega$ is enhanced from $2\alpha\Omega_r$ into $(2\alpha + \kappa)\Omega_r$. The origin lies on \mathcal{T}_e^L , which is triggered by the induced spin, where the spin is induced by the magnetization dynamics on the surface of the doped TI. This enhancement of $\Delta\Omega$ has been verified in the recent experiment²⁸.

We compare $\Delta\Omega$ in MI/TI junction with $\Delta\Omega$ in FM/NM junction. In the FM/NM junction, it has been demonstrated that the enhancement of $\Delta\Omega$ is triggered by the spin current in the NM, which is generated by the magnetization dynamics of the FM⁴⁴. On the surface of the MI/TI junction with uniform spin structure, on the other hand, spin current is not generated by magnetization dynamics, and the spin current does not contribute to $\Delta\Omega$. The enhancement of $\Delta\Omega$ is caused by the spin polarization due to the magnetization dynamics on the surface.

C. Magnetic permeability with diffusion

We will consider the surface of the TI/MI junction, where the localized spin in the MI is spatially inhomogeneous. The spin structure of the localized spin we consider is a spin-wave or longitudinal conical spin structure, which are realized in ferrimagnetic insulator yttrium iron garnets (YIG) or multiferroics⁴⁵, respectively. We expect that even on the surface of the TI, the localized spin depends on the position through proximity effects from the MI. Then, if we apply ac magnetic field of microwave in the junction along the y direction, we assume that the localized spin becomes precessional motion by the applied magnetic field. The localized spin on the surface of the TI can be described by

$$\mathbf{S}(\mathbf{x}, t) = [S \cos(\mathbf{q} \cdot \mathbf{x} - \Omega t), S_y, S \sin(\mathbf{q} \cdot \mathbf{x} - \Omega t)], \quad (62)$$

where, S and S_y are a constant coefficient independent of space. We assume $|S| \ll |S_y|$ and $|\mathbf{S}| \sim S_y$. Here $\mathbf{q} = (q_x, q_y)$ is the momentum of the localized spin and is assumed to be monochromatic. The direction and the magnitude of \mathbf{q} depends on materials of the MI. In the spin structure, nonlocal diffusive spin $\langle \mathbf{S} \rangle_D$ is given by Eqs. (27) and (62) as

$$\begin{aligned} \langle S_x \rangle_D &= A_{q,\Omega} S \cos[\mathbf{q} \cdot \mathbf{x} - \Omega t] - B_{q,\Omega} S \sin[\mathbf{q} \cdot \mathbf{x} - \Omega t], \\ \langle S_z \rangle_D &= B_{q,\Omega} S \cos[\mathbf{q} \cdot \mathbf{x} - \Omega t] + A_{q,\Omega} S \sin[\mathbf{q} \cdot \mathbf{x} - \Omega t]. \end{aligned} \quad (63)$$

The component of $\langle \mathbf{S} \rangle_D$ is different from that of \mathbf{S} : $\langle S_x \rangle_D$ has $\cos[\mathbf{q} \cdot \mathbf{x} - \Omega t]$ components, as well as $\sin[\mathbf{q} \cdot \mathbf{x} - \Omega t]$ components. Here, the coefficients A and B are obtained (see Appendix A) as

$$A_{q,\Omega} = \frac{q^2 \ell^2}{(\Omega \tau)^2 + (q^2 \ell^2)^2}, \quad (64)$$

$$B_{q,\Omega} = \frac{\Omega \tau}{(\Omega \tau)^2 + (q^2 \ell^2)^2}. \quad (65)$$

The coefficients $A_{q,\Omega}$ and $B_{q,\Omega}$ depend on $q\ell$ and $\Omega\tau$, where parameters ℓ and τ are determined by the TI, and q and Ω are chosen as characteristic values of the MI. Then, the diffusive spin \mathbf{s}^D is given from Eqs. (39) as

$$\mathbf{s}^D = \nu_e J_{sd} \tau \ell^2 [q^2 \partial_t \langle \mathbf{S}^{\parallel} \rangle_D - \mathbf{q}(\mathbf{q} \cdot \partial_t \langle \mathbf{S}^{\parallel} \rangle_D)]. \quad (66)$$

Then, nonlocal diffusive spin torque \mathcal{T}_e^D is obtained by using $\langle \mathbf{M}^{\parallel} \rangle_D = -(M^{\parallel}/S^{\parallel}) \langle \mathbf{S}^{\parallel} \rangle_D$ as

$$\mathcal{T}_e^D = -\frac{\kappa \ell^2}{M^{\parallel}} [q^2 \mathbf{M} \times \partial_t \langle \mathbf{M}^{\parallel} \rangle_D - (\mathbf{M} \times \mathbf{q})(\mathbf{q} \cdot \partial_t \langle \mathbf{M}^{\parallel} \rangle_D)]. \quad (67)$$

The first term of Eq. (67) plays the role of an anisotropic damping torque, which is similar to \mathcal{T}_e^L . The direction of this torque is independent of the direction of \mathbf{q} . On the other hand, the second term of Eq. (67) is proportional to $(\mathbf{M} \times \mathbf{q})(\mathbf{q} \cdot \partial_t \langle \mathbf{M}^\parallel \rangle_D)$, and its direction depends on \mathbf{q} .

Using Eqs. (62)-(67), we consider the magnetic permeability affected by \mathcal{T}_e^D . Then, the LLG equation is given within the linear order of the magnetization as

$$\begin{aligned}\partial_t m_x &= \omega_H m_z - h_z \omega_M + \alpha \partial_t m_z \\ \partial_t m_z &= h_x \omega_M - \omega_H m_x - (\alpha + \kappa) \partial_t m_x + \kappa q_y^2 \ell^2 \partial_t \langle M^{\parallel, x} \rangle_D.\end{aligned}$$

The last term of the above equation is caused by \mathcal{T}_e^D . In order to discuss the permeability due to \mathcal{T}_e^D , we consider when the momentum has the y -component ($\mathbf{q} = q\mathbf{y}$), whose direction is parallel to the applied static magnetic field. That means that the spin structure we consider is a longitudinal conical spin structure. From the above equation, using $\langle M^{\parallel, x} \rangle_D = A_{q, \Omega} m_x - B_{q, \Omega} m_z$, we obtain the magnetic permeability as

$$\begin{pmatrix} m_x \\ m_z \end{pmatrix} = \begin{pmatrix} \chi_{xx}^D & \chi_{xz}^D \\ \chi_{zx}^D & \chi_{zz}^D \end{pmatrix} \begin{pmatrix} h_x \\ h_z \end{pmatrix}. \quad (68)$$

Here the longitudinal and transverse magnetic permeability are given by

$$\chi_{xx}^D(q, \Omega) = \frac{(\omega_H + i\alpha\Omega)\omega_M}{[\omega_H + i\alpha\Omega][\omega_H + i(\alpha + \tilde{\kappa}_{q, \Omega})\Omega] - \zeta_{q, \Omega}\Omega^2}, \quad (69)$$

$$\chi_{zz}^D(q, \Omega) = \frac{\omega_H + i(\alpha + \tilde{\kappa}_{q, \Omega})\Omega}{\omega_H + i\alpha\Omega} \chi_{xx}^D, \quad (70)$$

$$\chi_{xz}^D(q, \Omega) = -\zeta_{q, \Omega} \chi_{zx}^D. \quad (71)$$

The obtained permeability is different from that in Eqs. (58)-(60). The difference is caused by coefficients $\tilde{\kappa}_{q, \Omega}$ and $\zeta_{q, \Omega}$:

$$\tilde{\kappa}_{q, \Omega} = \kappa(1 - q^2 \ell^2 A_{q, \Omega}), \quad (72)$$

$$\zeta_{q, \Omega} = 1 + \kappa q^2 \ell^2 B_{q, \Omega}. \quad (73)$$

The $\tilde{\kappa}_{q, \Omega}$ and $\zeta_{q, \Omega}$ depend on $q\ell$ and $\Omega\tau$. If $q = 0$, one can demonstrate $\tilde{\kappa}_{q, \Omega} = \kappa$ and $\zeta_{q, \Omega} = 1$, and the magnetic permeability in Eqs. (69)-(71) equal to that in Eqs. (58)-(60), respectively. Figure 2(a) indicates the $\Omega\tau$ dependence of $\tilde{\kappa}/\kappa$ for several momentum $q\ell$. The parameter $\tilde{\kappa}/\kappa$ approaches to 0 from $\tilde{\kappa}/\kappa = 1$ with increasing $\Omega\tau$: In the case for $\tilde{\kappa}/\kappa = 0$,

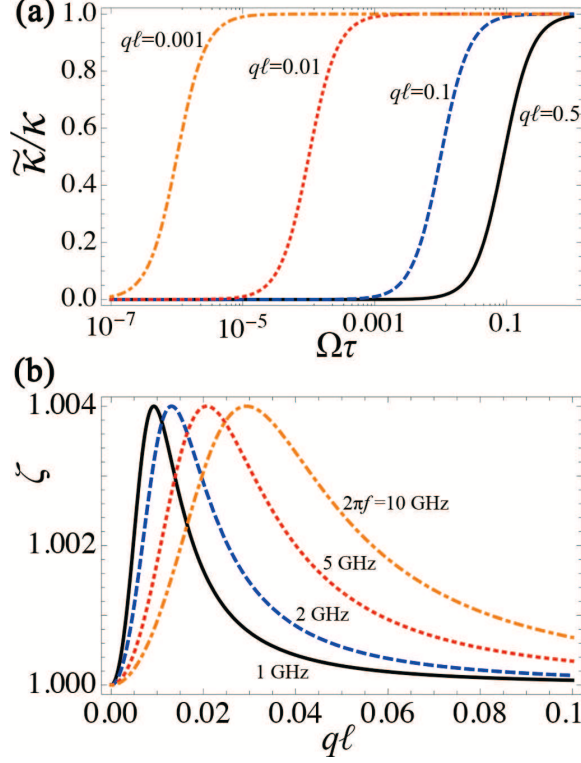


FIG. 2: (Color online) (a) The $\Omega\tau$ dependence of $\tilde{\kappa}/\kappa$ for several $q\ell$. (b) The $q\ell$ dependence of the ζ for several frequency ($2\pi f = 1, 2, 5, 10$ GHz) in the fixed relaxation time ($\tau = 0.087$ ps).

\mathcal{T}_e^L and \mathcal{T}_e^D are canceled out each other, and the spin torque \mathcal{T}_e vanishes. On the other hand, $\tilde{\kappa}/\kappa = 1$ means that \mathcal{T}_e^D is zero and \mathcal{T}_e^L is nonzero. The relation $\tilde{\kappa}/\kappa$ significantly changed when $(q\ell)^2 \sim \Omega\tau$ is satisfied. Figure 2(b) shows the $q\ell$ dependence of ζ for several angular frequency of the applied ac magnetic field Ω , where we take a realistic relaxation time ($\tau = 0.087$ ps⁴⁶). The magnitude of ζ changes around $q\ell \sim \sqrt{\Omega\tau}$ and approaches to $\zeta = 1$ with increasing $q\ell$.

Figure 3 (a) and (b) show the $\Omega\tau$ dependence of the real and imaginary part of the longitudinal magnetic permeability, $\text{Re}[\chi_{xx}^D]$ and $-\text{Im}[\chi_{xx}^D]$, respectively. In Figs. 3(a) and (b), we choose realistic parameters of the TI: $\ell = 40\text{nm}$, $v_F = 4.6 \times 10^5\text{m/s}$ ⁴⁶, $\tau = 0.087$ ps, $\xi = 0.003$, and $\tilde{v}_F/v_F = 0.997$. Besides, we choose material parameters of the ferromagnets²⁸: $\alpha = 0.015$, $J_{sd} \sim 6\text{meV}$, $S^\parallel \sim 0.3$, and Fermi wavenumber $k_F = 3.9 \times 10^8\text{m}^{-1}$. Then, $\kappa = 0.008$ is obtained. The frequency of the magnetization $\omega_M/(2\pi) = f_M = 0.28$ GHz in the MI. The magnitude of the frequency is evaluated by the material parameters of the permalloy²⁸.

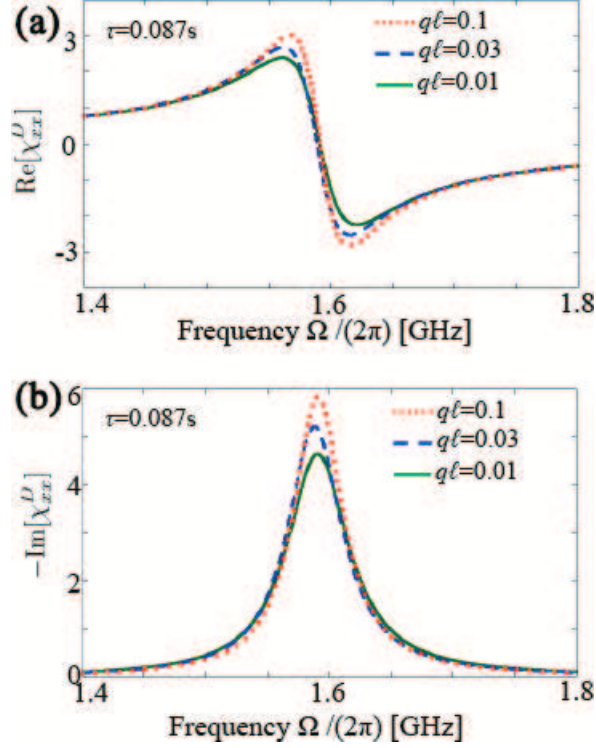


FIG. 3: (Color online) (a)-(b) The frequency dependence of the real part and imaginary part of the longitudinal permeability, $\text{Re}[\chi_{xx}^D]$ and $-\text{Im}[\chi_{xx}^D]$, for a fixed Gilbert damping constant ($\alpha = 0.015$), the relaxation time [$\tau = 0.087\text{ps}$], the anisotropic damping constant [$\kappa = 0.008$], and the frequency [$f_H = 1.6\text{ GHz}$ and $f_M = 0.28\text{ GHz}$] for several momentum $q\ell$.

We plot the $\text{Re}[\chi_{xx}^D]$ and $-\text{Im}[\chi_{xx}^D]$ functions as the frequency of the ac magnetic field for several momentum of the localized spin, when we take the frequency of the static magnetic field $\omega_H/(2\pi) = f_H = 1.6\text{ GHz}$. The magnitude of $\Omega\tau$ can be estimated as $\Omega\tau \sim \omega_H\tau = 8.6 \times 10^{-3}$. For $q\ell < 0.03$, the permeability $\text{Re}[\chi_{xx}^D]$ and $-\text{Im}[\chi_{xx}^D]$ are not dramatically changed from that without diffusion, $\text{Re}[\chi_{xx}]$ and $-\text{Im}[\chi_{xx}]$, respectively. The reason is due to the profile of $\tilde{\kappa}/\kappa$ and ζ : Both $\tilde{\kappa}/\kappa$ and ζ are about 1 within $q\ell < 0.03$ in $\Omega\tau \sim 8.6 \times 10^{-3}$. While $q\ell$ is near $q\ell = 0.03$, χ_{xx}^D changes: The magnitude of χ_{xx}^D increases from that of χ_{xx} . Besides, the resonant frequency of χ_{xx}^D increases from that of χ_{xx} [see $q\ell = 0.03$ in Figs. 3 (a)-(b)]. The change of the resonant frequency is also shown in Fig. 4 (a). We find that when $(q\ell)^2 \sim \Omega\tau$ is satisfied, $\tilde{\kappa}/\kappa$ and ζ deviate from 1, as shown in Figs. 2(a)-(b). After increasing $q\ell$ from $q\ell = 0.03$, the shifted resonant frequency gets back again. The magnitude of the permeability increases with increasing $q\ell$.

The half-width value is also changed by the magnitude of $\text{Im}[\chi_{xx}^D]$ for several momentum

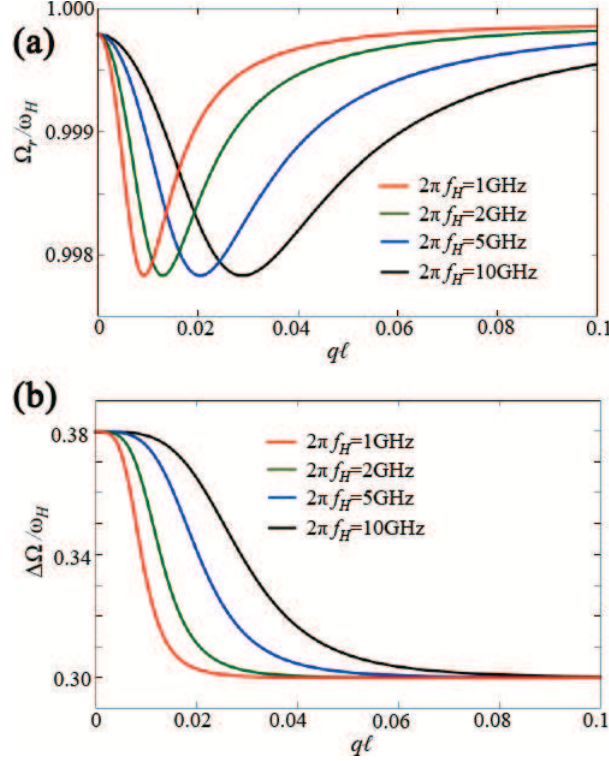


FIG. 4: (Color online) The $q\ell$ dependence of the resonant frequency (a) and the half-width value (b) normalized by the angular frequency of the applied magnetic field for several frequencies ($2\pi f_H = 1, 2, 5$, and 10 GHz) in $2\alpha + \kappa = 0.038$ and $2\alpha = 0.030$.

$q\ell$. This trade off between the half-width value and $q\ell$ for several frequency ($2\pi f_H = 1, 2, 5$, and 10 GHz) is shown in Fig. 4(b). In the case for $\tau = 0.087$ ps, the half-width value $\Delta\Omega$ significantly changed around the $q\ell$, which satisfies $q\ell \sim \sqrt{\Omega\tau}$ (e.g., $q\ell = 0.03$ in $\omega_H = 10$ GHz). Figure 4(a) indicates $q\ell$ dependence of the resonant frequency rate Ω_r/ω_H . The Ω_r/ω_H changed from $\Omega_r/\omega_H \sim 1$ into $\Omega_r/\omega_H = 0.998$ around the $q\ell$, which satisfies $q\ell \sim \sqrt{\Omega\tau}$.

We discuss the role of diffusive spin torque \mathcal{T}_e^D from Figs. 4(a) and (b). Figure 4(a) shows that the resonant angular frequency Ω_r tends to decrease with increasing $q\ell$. The decrease of Ω_r can be caused by the increase of $\zeta_{q,\Omega}$, and the change of $\zeta_{q,\Omega}$ is caused by \mathcal{T}_e^D . Therefore, we expect that \mathcal{T}_e^D plays a role as a field-like torque to shift the resonant frequency. Then, Fig.4 (b) indicates that the half-width value tends to decrease with increasing $\tilde{\kappa}_{q,\Omega}$ in Eq. (73), which is caused by \mathcal{T}_e^D . It means that the damping of the magnetization dynamics is reduced by \mathcal{T}_e^D on the disordered surface of the doped TI. Thus, \mathcal{T}_e^D behaves

TABLE I: A brief summary of the role of the spin torques and the half-width value in several spin structures on the surface of the TI, when the direction of \mathbf{H}_0 and the propagation of \mathbf{H}_{ac} are parallel to y -axis.

	Uniform	Transverse conical ($q_y = 0$)	Longitudinal conical ($q_y \neq 0$)
\mathcal{T}_e^L	Damping torque	Damping torque	Damping torque
\mathcal{T}_e^D	–	–	Damping torque and field-like torque
$\Delta\Omega/\Omega_r$	$2\alpha + \kappa$	$2\alpha + \kappa$	$2\alpha + \tilde{\kappa}$

both the damping torque and the field-like torque. The role of the spin torque in several spin structures are summarized in the Table I. From the table I, we can expect to distinguish the half-width value contributed from \mathcal{T}_e^L and \mathcal{T}_e^D by tuning of the magnitude of the applied magnetic field \mathbf{H}_0 . The reason is why the longitudinal spin structure changes an spatial uniform ferromagnetic structure if when we apply a strong magnetic field, which broke the longitudinal spin structure. Then, $q\ell$ of the spatial uniform spin structure can be regarded as $q\ell = 0$. Therefore, we expect that if when we apply the strong applied magnetic field in the longitudinal spin structure, the half-width value with a finite $q\ell$ changes into the half-width value with $q\ell = 0$ as $\Delta\Omega/\Omega_r = 2\alpha + \tilde{\kappa} \rightarrow 2\alpha + \kappa$ [see Fig.4 (b)].

For magnetization dynamics due to the magnetic resonance, we need to apply magnetic fields in the MI/TI junction. Then, the spin-charge generation and transport are triggered not only by the magnetization dynamics, but also by the applied magnetic field. We will estimate when the contribution due to the magnetic field can be relevant. The contribution from the applied magnetic field can be described by the Zeeman effect, $\mathcal{H}_Z = -2\hbar\gamma \int d\mathbf{x} \mathbf{B} \cdot \mathbf{s}$, where \mathbf{B} is the applied magnetic field and couples with conduction electrons spin on the surface of the TI. The contribution from \mathbf{B} can be treated within the same formalism in sections 3 and 4 by replacing $\mathbf{S} \rightarrow \mathbf{S} + 2(\hbar\gamma/J_{sd})\mathbf{B}$ in Eq. (3). As a result, the spin-charge generation and transport due to \mathcal{H}_Z and \mathcal{H}_{sd} are obtained by replacing $\mathbf{S} \rightarrow \mathbf{S} + 2(\hbar\gamma/J_{sd})\mathbf{B}$ in Eqs. (26), (31), (38)-(39), and (42)-(43). We expect that the contribution from \mathcal{H}_Z can be ignored compared with that from \mathcal{H}_{sd} , when the energy scale of the Zeeman effect is smaller than that of the exchange energy on the surface of the TI as $2\hbar\gamma|\mathbf{B}|/(J_{sd}|\mathbf{S}|) \ll 1$. The $|\mathbf{B}|/J_{sd}$ value can be estimated by $|\mathbf{B}|/J_{sd} \ll 1/(2\hbar\gamma) \sim 4 \times 10^4 \text{ T}\cdot\text{eV}^{-1}$ in $\mathbf{S} \sim 1$. Then, the

magnitude of the exchange coupling J_{sd} can be estimated. Using realistic parameters, the mean-free path $\ell = 40\text{nm}$, Fermi velocity $v_F = 4.6 \times 10^5\text{m/s}$ ⁴⁶, we obtain the $\hbar/\tau \sim 15\text{meV}$ and $J_{sd} \ll 15\text{ meV}$, which is requested for the perturbation condition $J_{sd}\tau/\hbar \ll 1$. Then, if $|\mathbf{B}| \gg 10\text{T}$ is satisfied, we need to consider the contribution from \mathcal{H}_Z .

At the end of this section, we estimate the spin density due to the dynamics of the longitudinal spin structure $\mathbf{S} = S^\parallel(\sin\theta \cos\Omega t, 1, \sin\theta \sin\Omega t)$ in the case of $\theta \ll 1$ around resonance angular frequency $\Omega \sim 1 \times 10^{10}\text{s}^{-1}$. The magnitude of the spin depends on the regime of $q^2\ell^2 \ll \Omega\tau$ or $q^2\ell^2 \gg \Omega\tau$. In $q^2\ell^2 \ll \Omega\tau$ regime, the magnitude of the nonlocal spin can be negligible small compared with that of the local term, and the spin is estimated by $|\mathbf{s}| \sim 1.6 \times 10^{-10}\text{\AA}^{-2}$ at $\theta \sim 0.1\text{ rad}$ in the FMR. Then, we find that the magnitude of the spin due to the spin-pumping is smaller than that of the spin due to the applied electric field⁴⁷. On the other hand, in $q^2\ell^2 \gg \Omega\tau$ regime, the local and nonlocal spin vanishes each other even in the presence of FMR. From the results, we expect that the change of the magnitude of the spin dependent on $q^2\ell^2/\Omega\tau$ can be measurable for several applied magnetic fields, because the inhomogenous spin structure ($q\ell \neq 0$) changes into an uniform spin structure ($q\ell \sim 0$) by using an applied strong magnetic field.

D. Spin current and charge current

We will discuss the spin current on the surface of the disordered MI/TI junction compared with that in the FM/NM junction. The spin current due to the spin-pumping $j_{i,\text{FM/NM}}^\alpha$ in the FM/NM junction is triggered by the magnetization dynamics as^{1,2,5}

$$j_{i,\text{FM/NM}}^\alpha = b\nabla_i\partial_t S^\alpha + \mathcal{O}(S^2), \quad (74)$$

where b is a coefficient dependent on materials. It is similar to the spin current in Eq. (74), that the spin current is proportional to a time-dependent magnetization and the spin current vanishes when the magnetization is spatially uniform. The direction of the spin (α) and the flow (i) of the spin current in Eq. (74) are not related each other. On the other hand, spin current on the surface of the TI, whose direction of spin and flow are perfectly perpendicular to each other. The difference lies on the spin-orbit interaction. The j_i^α in Eq. (31) includes the contribution of the spin-orbit interaction, which is absent in Eq. (74) does not.

Charge current due to the spin-pumping in the FM/NM junction is also given by the

magnetization dynamics and Rashba type spin-orbit interactions. When the magnetization is spatially uniform, the charge current $\mathbf{j}_{\text{FM/NM}}$ becomes^{2,5}

$$\mathbf{j}_{\text{FM/NM}} = \boldsymbol{\alpha} \times (\mathbf{S} \times \partial_t \mathbf{S}), \quad (75)$$

where $\boldsymbol{\alpha}$ is a constant vector including the contribution from the spin-orbit interaction. The charge current in Eq. (75) is proportional to the second-order of the localized spin \mathbf{S} . That is different from the charge current on the surface of TIs. The charge current on the surface of the TI is proportional to the localized spin $\partial_t \mathbf{S}^\parallel$, as shown in Eq. (43). The difference is due to the property of the localized spin: the localized spin plays the role of the effective vector potential on the surface of the TI. We note that the frequency dependence of these charge current is also different; $\mathbf{j}_{\text{TI}} \propto \partial_t \mathbf{S}^\parallel$ oscillates with time of the localized spin in the FMR, but $\mathbf{j}_{\text{FM/NM}} \propto \mathbf{S} \times \partial_t \mathbf{S}$ does not. For example, the ac current $\mathbf{j}_{\text{TI}} \propto (\cos \Omega t, \sin \Omega t, 0)$ is given when we apply the magnetic field parallel to the z direction on the TI/MI junction. On the other hand, the dc current $\mathbf{j}_{\text{FM/NM}} \propto \Omega(0, 0, 1)$ is obtained when we apply the magnetic field parallel to the z direction in the NM/FM junction.

VI. SUMMARY

We have studied the spin-charge generation and transport due to the magnetization dynamics on the disordered surface of the doped TI/MI junction. The spin current $j_{s,i}^\alpha$ is proportional to the charge density ρ_e and the direction of its spin and its flow are perfectly perpendicular to each other, because of the spin-momentum locking on the surface of the TI. We have found that j_i^α and ρ_e are induced by the time- and spatial-dependent of nonlocal magnetization dynamics, which is affected by nonmagnetic impurity scatterings on the disordered surface of the doped TI. These results of j_i^α and ρ_e are shown in Eqs. (31) and (26), respectively. j_i^α and ρ_e is induced except when the magnetization dynamics is spatially uniform. We have also shown the induced spin \mathbf{s} and charge current density \mathbf{j} due to the magnetization dynamics. Because of the spin-momentum locking, the spin \mathbf{s} and charge current density \mathbf{j} are proportional to each other. The \mathbf{s} and \mathbf{j} are generated not only by the local magnetization dynamics, but also by the nonlocal magnetization dynamics with the diffusion on the disordered surface of the doped TI. These results of \mathbf{s} and \mathbf{j} are shown in Eqs. (38)-(39) and (42)-(43), respectively. A brief summary of the local and nonlocal ρ_e ,

TABLE II: A brief summary of the charge, charge current, spin, and spin current density due to the magnetization dynamics on the disordered surface of the TI. These terms are driven by the effective electric field \mathcal{E} .

	charge density ρ_e	current density j_i	spin density s^α	spin current density j_i^α
Local term	–	$\mathbf{z} \times \partial_t \mathbf{S}^\parallel$	$\partial_t \mathbf{S}^\parallel$	–
Nonlocal term	$[\nabla \times \partial_t \langle \mathbf{S}^\parallel \rangle_D]_z$	$\nabla[\nabla \times \partial_t \langle \mathbf{S}^\parallel \rangle_D]_z$	$(\mathbf{z} \times \nabla)[\nabla \times \partial_t \langle \mathbf{S}^\parallel \rangle_D]_z$	$[\nabla \times \partial_t \langle \mathbf{S}^\parallel \rangle_D]_z$
Driving field	$\nabla \cdot \langle \mathcal{E} \rangle_D$	$\mathcal{E}, \nabla^2 \langle \mathcal{E} \rangle_D$	$\mathbf{z} \times \mathcal{E}, (\mathbf{z} \times \nabla)[\nabla \cdot \langle \mathcal{E} \rangle_D]$	$\nabla \cdot \langle \mathcal{E} \rangle_D$

j_i^α , \mathbf{s} , and \mathbf{j} due to the magnetization dynamics are represented in Table. II. As a result, we have discussed the modification of the magnetization dynamics before and after these spin-charge generation and transport on the disordered surface of the doped TI. These spin-charge generation and transport can be detected from the half-width value of the magnetic permeability in the magnetic resonance in the MI/TI junction, as discussed in section V. The magnitude of a Gilbert damping constant α in ferromagnetic insulator is smaller than that in ferromagnetic metals. Then, we can easily detect the change of the f_H dependence of the resonant frequency and half-width value, which are shown in Figs. 4 (a)-(b).

The preparation of the hybrid system with the ferromagnetic insulator deposited on the surface of the TI, EuS/Bi₂Se₃, has been reported⁵⁰, where the magnetic moment of Eu locates at the interface between the EuS and Bi₂Se₃. If the magnetization dynamics of the magnetic moment of Eu is triggered by an applied magnetic field, the spin density and charge current can be induced on the surface of the TI. Additionally, the magnetic distribution of Eu has a magnetic domain, which is spatially dependent on the position on the surface. Therefore, when we move the magnetic domain by using an applied magnetic field, the charge density and the spin current are also triggered only around the magnetic domain. Recently, magnetic insulator with noncoplanar spin structure has been reported. For example, magnetoelectric insulator Cu₂OSeO₃ has spatially dependent spin structure, and is called skyrmion, which is topologically protected magnetic spin vortex-like object^{51,52}. If one can prepare the vortex-like spin structure deposited on the surface of the TI and can trigger the magnetization dynamics of the skyrmion, we expect that the charge and spin

currents are driven by the magnetization dynamics of the skyrmion. Moreover, the spatial distributions of the charge density and the magnitude of the spin current depends on the position of the skyrmion, because the spatial derivative of the localized spin depends on the positions in the skyrmion. We comment that the induced spin and charge currents could be independent of the polarity of the skyrmion, since these current are triggered by the in-plane component of the localized spin [see Eqs. (31) and (42)-(43)]. Then, we expect that in the MIs deposited on the surface of the TI, the magnetization dynamics induces not only the local spin-charge generation and transport, but also the diffusive one. Our obtained results will enable the applications of TI nanomembrane in spintronics devices.

ACKNOWLEDGEMENTS

The authors would like to thank A. A. Golubov, A. Dutt, and A. Yamakaga for valuable discussions. This work was supported by Grants-in-Aid for Young Scientists (B) (No. 22740222 and No. 23740236), by Grants-in-Aid for Scientific Research on Innovative Areas “Topological Quantum Phenomena” (No. 22103005 and No. 25103709) from the Ministry of Education, Culture, Sports, Science, and Technology, Japan (MEXT), and by the Core Research for Evolutional Science and Technology (CREST) of the Japan Science. K.T. acknowledges support from a Grant-in-Aid for Japan Society for the Promotion of Science (JSPS) Fellows.

Appendix A: Derivation of Eqs. (65)-(66)

We show details of calculation of coefficient $A_{q,\Omega}$ and $B_{q,\Omega}$ of nonlocal localized spin $\langle \mathbf{S} \rangle_D$. The $\langle \mathbf{S} \rangle_D$ is given by

$$\langle \mathbf{S} \rangle_D(\mathbf{x}, t) \equiv \iint dt' d\mathbf{x}' \mathcal{D}(\mathbf{x} - \mathbf{x}', t - t') \mathbf{S}(\mathbf{x}', t') \quad (\text{A1})$$

To substitute $\mathbf{S} = S(1, 0, -i)e^{i(\mathbf{q} \cdot \mathbf{x} - \Omega t)} \propto e^{i(\mathbf{q} \cdot \mathbf{x} - \Omega t)}$ into the above equation, we calculate $\langle n \rangle_D$:

$$\begin{aligned} \langle n \rangle_D &= \frac{1}{L^2} \iint dt' d\mathbf{x}' \sum_{Q, \omega} \frac{e^{i[\omega(t-t') - \mathbf{Q} \cdot (\mathbf{x} - \mathbf{x}')] } e^{i(\mathbf{q} \cdot \mathbf{x}' - \Omega t')}}{Q^2 \ell^2 + i\omega\tau} \\ &= \frac{e^{i(\mathbf{q} \cdot \mathbf{x} - \omega t)}}{q^2 \ell^2 - i\Omega\tau} \end{aligned} \quad (\text{A2})$$

The resulting $\langle S^x \rangle_D$ is obtained from the real part of $S\langle n \rangle_D$ in the above equation. In the same way, $\langle S^z \rangle_D$ is obtained from the real part of $-iS\langle n \rangle_D$. Thus, from the above equation, the coefficient of $A_{q,\Omega}$ and $B_{q,\Omega}$ are derived as Eqs. (65)-(66).

Appendix B: Charge conservation

To check the validity of the spin current and the charge current we calculate, we use the charge conservation law $\partial_t \rho_e + \nabla \cdot \mathbf{j} = 0$. The charge density $\partial_t \rho_e$ is given by

$$\partial_t \rho_e = \frac{e\nu_e J_{sd}\tau}{L^2} \left[\sum_{\mathbf{q},\Omega} e^{i[\Omega t - \mathbf{q} \cdot \mathbf{x}]} \frac{i\ell\Omega^2}{q^2\ell^2 + i\Omega\tau} (q_y S_{\mathbf{q},\Omega}^x - q_x S_{\mathbf{q},\Omega}^y) \right], \quad (\text{B1})$$

where $\ell = \tilde{v}_F \tau$ is the mean-free path. The resulting $\nabla \cdot \mathbf{j}$ becomes

$$\begin{aligned} \nabla_x j_x &= \frac{e\tilde{v}_F \nu_e J_{sd}\tau}{L^2} \sum_{\mathbf{q},\Omega} e^{i[\Omega t - \mathbf{q} \cdot \mathbf{x}]} \Omega \left[\left\{ 1 - \frac{1}{2} \frac{q^2 \ell^2}{q^2 \ell^2 + i\Omega\tau} \right\} q_x S_{\mathbf{q},\Omega}^y + \frac{1}{2} \frac{\ell^2 q^2}{\ell^2 q^2 + i\Omega\tau} q_y S_{\mathbf{q},\Omega}^x \right], \\ \nabla_y j_y &= -\frac{e\tilde{v}_F \nu_e J_{sd}\tau}{L^2} \sum_{\mathbf{q},\Omega} e^{i[\Omega t - \mathbf{q} \cdot \mathbf{x}]} \Omega \left[\left\{ 1 - \frac{1}{2} \frac{q^2 \ell^2}{q^2 \ell^2 + i\Omega\tau} \right\} q_y S_{\mathbf{q},\Omega}^x + \frac{1}{2} \frac{\ell^2 q^2}{\ell^2 q^2 + i\Omega\tau} q_x S_{\mathbf{q},\Omega}^y \right], \end{aligned}$$

and

$$\begin{aligned} \nabla_x j_x + \nabla_y j_y &= \frac{e\tilde{v}_F \nu_e J_{sd}\tau}{L^2} \sum_{\mathbf{q},\Omega} e^{i[\Omega t - \mathbf{q} \cdot \mathbf{x}]} \Omega \left[\left\{ 1 - \frac{q^2 \ell^2}{q^2 \ell^2 + i\Omega\tau} \right\} (q_x S_{\mathbf{q},\Omega}^y - q_y S_{\mathbf{q},\Omega}^x) \right] \\ &= \frac{e\nu_e J_{sd}\tau}{L^2} \sum_{\mathbf{q},\Omega} e^{i[\Omega t - \mathbf{q} \cdot \mathbf{x}]} \left[\frac{i\Omega^2 \tilde{v}_F \tau}{q^2 \ell^2 + i\Omega\tau} (q_x S_{\mathbf{q},\Omega}^y - q_y S_{\mathbf{q},\Omega}^x) \right] = -\partial_t \rho_e. \end{aligned} \quad (\text{B2})$$

Therefore, the ρ_e and \mathbf{j} satisfy $\partial_t \rho_e + \nabla \cdot \mathbf{j} = 0$.

-
- ¹ Y. Tserkovnyak, A. Brataas, and G. E. W. Bauer, *Spin pumping and magnetization dynamics in metallic multilayers*, Phys. Rev. Lett. **88**, 117601 (2002).
 - ² J.-I. Ohe, A. Takeuchi, and G. Tatara, *Charge Current Driven by Spin Dynamics in Disordered Rashba Spin-Orbit System*, Phys. Rev. Lett. **99**, 266603 (2007).
 - ³ E. Saitoh, M. Ueda, H. Miyajima, and G. Tatara, *Conversion of spin current into charge current at room temperature: Inverse spin-Hall effect*, Appl. Phys. Lett. **88**, 182509 (2006).
 - ⁴ A. Stern, *Berry's phase, motive forces, and mesoscopic conductivity*, Phys. Rev. Lett. **68** 1022 (1992).

- ⁵ A. Takeuchi and G. Tatara, *Charge and Spin Currents Generated by Dynamical Spins*, J. Phys. Soc. Jpn. **77**, 074701 (2008).
- ⁶ M. Z. Hasan and C. L. Kane, *Colloquium: Topological insulators*, Rev. Mod. Phys. **82**, 3045 (2010).
- ⁷ X.-L. Qi and S.-C. Zhang, *Topological insulators and superconductors*, Rev. Mod. Phys. **83**, 1057 (2011).
- ⁸ Y. Ando, *Topological Insulator Materials*, J. Phys. Soc. Jpn. **82**, 102001 (2013).
- ⁹ L. Fu and C. L. Kane, *Superconducting Proximity Effect and Majorana Fermions at the Surface of a Topological Insulator*, Phys. Rev. Lett. **100**, 096407 (2008).
- ¹⁰ A. R. Akhmerov, J. Nilsson, and C. W. J. Beenakker, *Electrically Detected Interferometry of Majorana Fermions in a Topological Insulator*, Phys. Rev. Lett. **102**, 216404 (2009).
- ¹¹ Y. Tanaka, T. Yokoyama and N. Nagaosa, *Manipulation of the Majorana Fermion, Andreev Reflection, and Josephson Current on Topological Insulators*, Phys. Rev. Lett. **103**, 107002 (2009).
- ¹² X.-L. Qi, T. L. Hughes, and S.-C. Zhang, *Topological field theory of time-reversal invariant insulators*, Phys. Rev. B **78**, 195424 (2008).
- ¹³ K. Nomura and N. Nagaosa, *Electric charging of magnetic textures on the surface of a topological insulator*, Phys. Rev. B **82**, 161401 (2010).
- ¹⁴ H. T. Ueda, A. Takeuchi, G. Tatara, and T. Yokoyama, *Topological charge pumping effect by the magnetization dynamics on the surface of three-dimensional topological insulators*, Phys. Rev. B **85**, 115110 (2012).
- ¹⁵ I. Garate and M. Franz, *Magnetoelectric response of the time-reversal invariant helical metal*, Phys. Rev. B **81**, 172408 (2010).
- ¹⁶ T. Yokoyama, Y. Tanaka, and N. Nagaosa, *Anomalous magnetoresistance of a two-dimensional ferromagnet/ferromagnet junction on the surface of a topological insulator*, Phys. Rev. B, **81**, 121401(R) (2010).
- ¹⁷ S. Mondal, D. Sen, K. Sengupta, and R. Shankar, *Magnetotransport of Dirac fermions on the surface of a topological insulator*, Phys. Rev. B. **82**, 045120 (2010).
- ¹⁸ B. D. Kong, Y. G. Semenov, C. M. Krowne, and K. W. Kim, *Unusual magnetoresistance in a topological insulator with a single ferromagnetic barrier*, App. Phys. Lett. **98**, 243112 (2011).
- ¹⁹ D. Culcer, *Transport in three-dimensional topological insulators: Theory and experiment*, Phys-

- ica E, **44**, 860, (2012).
- ²⁰ M. J. Ma, M. B. A. Jalil, S. G. Tan, Y. Li, and Z. B. Siu, *Spin current generator based on topological insulator coupled to ferromagnetic insulators*, AIP Advances **2**, 032162 (2012)
 - ²¹ A. A. Burkov and D. G. Hawthorn, *Spin and Charge Transport on the Surface of a Topological Insulator*, Phys. Rev. Lett. **105**, 066802 (2010).
 - ²² P. Schwab, R. Raimondi, and C. Gorini, *Spin-charge locking and tunneling into a helical metal*, EPL (Europhysics Letters), **93**, 67004 (2011).
 - ²³ K. Taguchi, T. Yokoyama and Y. Tanaka, *Giant magnetoresistance in the junction of two ferromagnets on the surface of diffusive topological insulators*, Phys. Rev. B **89**, 085407 (2014).
 - ²⁴ T. Yokoyama, J. Zang, and N. Nagaosa, *Theoretical study of the dynamics of magnetization on the topological surface*, Phys. Rev. B **81**, 241410 (2010).
 - ²⁵ A. Sakai and H. Kohno, *Spin torques and charge transport on the surface of topological insulator*, Phys. Rev. B **89**, 165307 (2014).
 - ²⁶ A. R. Mellnik et al., *Spin-transfer torque generated by a topological insulator*, Nature (London) **511**, 449 (2014).
 - ²⁷ P. Deorani, J. Son, K. Banerjee, N. Koirala, M. Brahlek, S. Oh, and H. Yang, *Observation of inverse spin Hall effect in bismuth selenide*, Phys. Rev. B **90**, 094403 (2014).
 - ²⁸ Y. Shiomi, K. Nomura, Y. Kajiwara, K. Eto, M. Novak, Kouji Segawa, Yoichi Ando, and E. Saitoh, *Spin-Electricity Conversion Induced by Spin Injection into Topological Insulators*, Phys. Rev. Lett. **113** 196601 (2014).
 - ²⁹ M. Jamali, J.-S. Lee, Y. Lv, Z. Zhao, N. Samarth, and J.-P. Wang, *Room Temperature Spin Pumping in Topological Insulator Bi₂Se₃*, arXiv:1407.7940
 - ³⁰ X. Liu and J. Sinova, *Reading Charge Transport from the Spin Dynamics on the Surface of a Topological Insulator*, Phys. Rev. Lett. **111**, 166801 (2013).
 - ³¹ M. H. Fischer, A. Vaezi, A. Manchon, and E.-Ah Kim, *Large Spin Torque in Topological Insulator/Ferromagnetic Metal Bilayers*, arXiv:1305.1328.
 - ³² T. Yokoyama and Y. Tserkovnyak, *Spin diffusion and magnetoresistance in ferromagnet/topological-insulator junctions*, Phys. Rev. B **89**, 035408 (2014).
 - ³³ G. D. Mahan, *Many-Particle Physics*, 3rd ed. (Springer, 2000), p.514.
 - ³⁴ J. Fujimoto, A. Sakai, H. Kohno, *Ultraviolet divergence and Ward-Takahashi identity in a two-dimensional Dirac electron system with short-range impurities*, Phys. Rev. B **87**, 085437 (2013).

- ³⁵ Using $\frac{\hbar}{2\tau} = \frac{1}{2}\pi\nu_en_iu_0^2$, $\nu_e = \frac{\epsilon_F}{2\pi\hbar^2\tilde{v}_F^2}$, and $\tilde{v}_F/v_F = (1+\xi)^{-1}$, we can obtain the relation: $\xi(1+\xi)^2 = \frac{\hbar}{4\pi\epsilon_F\tau}$. Because of $\frac{\hbar}{\epsilon_F\tau} \ll 1$, $\xi < \frac{\hbar}{4\pi\epsilon_F\tau}$ becomes negligible small as $\tilde{v}_F/v_F = 1 + o(\frac{\hbar}{\epsilon_F\tau})$. Streakily speaking, there is no problem to take $\tilde{v}_F \simeq v_F$.
- ³⁶ If we do not take the replacement $v_F \rightarrow \tilde{v}_F$ in Eq. (2), the velocity operator on the surface of the TI becomes $\hat{v} = v_F(\mathbf{z} \times \hat{\boldsymbol{\sigma}})$. Then, the charge current is given by the multiple of v_F/\tilde{v}_F in Eqs. (42)-(43). The charge current does not satisfy the charge conservation law, which is shown in Appendix B.
- ³⁷ D. Culcer, J. Sinova, N. A. Sinitsyn, T. Jungwirth, A. H. MacDonald, and Q. Niu, *Semiclassical Spin Transport in Spin-Orbit-Coupled Bands*, Phys. Rev. Lett. **93**, 046602 (2004).
- ³⁸ J. Shi, P. Zhang, D. Xiao, and Q. Niu, *Proper Definition of Spin Current in Spin-Orbit Coupled Systems*, Phys. Rev. Lett. **96**, 076604 (2006).
- ³⁹ N. Nakabayashi, A. Takeuchi, K. Hosono, K. Taguchi, and G. Tatara, *Theory of spin relaxation torque in metallic ferromagnets*, Phys. Rev. B. **82**, 014403 (2010).
- ⁴⁰ H. Haug and A. P. Jauho, *Quantum Kinetics in Transport and Optics of Semiconductors*, 2nd ed. (Springer, New York, 2007), pp. 45–46.
- ⁴¹ $\hat{\Lambda}^{\text{ra}} = [1 - \tilde{\Gamma}^{\text{ra}}]^{-1}$ is given when $\max\{\sum_{\nu}[\tilde{\Gamma}^{\text{ra}}]_{\mu\nu}\} < 1$ is satisfied.
- ⁴² C. Kittel, *Introduction to Solid State Physics*, 8th ed. (Wiley, 2004), p.148.
- ⁴³ T. L. Gilbert, *A phenomenological theory of damping in ferromagnetic materials*, IEEE Trans. Magn. **40**, 3443 (2004).
- ⁴⁴ S. Mizukami, Y. Ando, and T. Miyazaki, *Effect of spin diffusion on Gilbert damping for a very thin permalloy layer in Cu/permalloy/Cu/Pt films*, Phys. Rev. B. **66**, 104413 (2002).
- ⁴⁵ Y. Tokura and N. Kida *Dynamical magnetoelectric effects in multiferroic oxides*, Phil. Trans. R. Soc. A **369**, 3679 (2011).
- ⁴⁶ A. A. Taskin, S. Sasaki, K. Segawa, and Y. Ando, *Manifestation of Topological Protection in Transport Properties of Epitaxial Bi₂Se₃ Thin Films*, Phys. Rev. Lett. **109**, 066803 (2012).
- ⁴⁷ T. Misawa, T. Yokoyama, and S. Murakami, , Phys. Rev. B. **84**, 165407 (2011).
- ⁴⁸ Y. Kajiwara et. al., *Transmission of electrical signals by spin-wave interconversion in a magnetic insulator*, Nature **464**, 262 (2010).
- ⁴⁹ I. Vobornik, U. Manju, J. Fujii, F. Borgatti, P. Torelli, D. Krizmancic, Y. S. Hor, R. J. Cava, and G. Panaccione, *Magnetic Proximity Effect as a Pathway to Spintronic Applications of Topological Insulators*, Nano Lett. **11**, 4079 (2011).

- ⁵⁰ P. Wei, F. Katmis, B.A. Assaf, H. Steinberg, P. Jarillo-Herrero, D. Heiman, J.S. Moodera, *Exchange-Coupling-Induced Symmetry Breaking in Topological Insulators*, Phys. Rev. Lett. **110**, 186807 (2013).
- ⁵¹ S. Seki, X. Z. Yu, S. Ishiwata, Y. Tokura, *bservation of Skyrmions in a Multiferroic Material*, science, **336** , 198 (2012).
- ⁵² J. S. White, et. al., *Electric-Field-Induced Skyrmion Distortion and Giant Lattice Rotation in the Magnetoelectric Insulator Cu₃OSeO₃*, Phys. Rev. Lett. **113**, 107203 (2014).